[long-term repopulating (LTR)-HSCs], CD34$^+$KSL (multipotential progenitor cells), c-kit$^+$ Sca1$^-$ lin$^-$ cells (progenitors), and their progeny subpopulations. Expression of *Roc1*, *Ddb1*, and *Cul4a* was detected in each of the hematopoietic subpopulations by RT-PCR analysis (Fig. 1*A*). Although *Cul4a* expression was predominant in lymphoid cells, that in HSC and progenitor subpopulations is presumed to be functionally significant because the HSC activity was reportedly defective in the heterozygous *Cul4a*-deficient mice (24). Because the yeast two-hybrid analysis with Hoxb4 as bait and Cul4a as prey clearly suggested that Hoxb4 directly interacts with Cul4a (Fig. S1*A*) similarly to Hoxa9 (25), we examined whether Hoxb4 forms a complex (designated as RDCOXB4) with Roc1-Ddb1-Cul4a in a cell line derived from the human kidney cells, HEK-293 cells (HEK-293), transfected with Flag-tagged Hoxb4. Roc1, Cul4a, and Ddb1 were detected in the immunoprecipitates prepared with an anti-Flag antibody (Fig. 1*B*), indicating that exogeneous Hoxb4 formed the RDCOXB4 complex in HEK-293. The similar complex formation was observed in a Hoxb4-transduced myeloid cell line, 32D cells (32D) (Fig. S1*B*). The RDCOXB4 complex may directly interact with Geminin because the yeast two-hybrid and immunoprecipitation analyses showed that Hoxb4 interacted with Geminin through the homeodomain (Fig. S1 *G* and *H*) as the other Hox proteins did (22).

Hoxb4 Restores Impaired HSC Activity and Geminin Protein Level in Rae$^{-/-}$FLC. We then determined whether Hoxb4 compensated for impaired HSC activity in Rae$^{-/-}$ mice, which resulted from accumulated Geminin (20). Hoxb4 was transduced into wild-type FLC (Rae$^{+/+}$FLC) and Rae$^{-/-}$FLC by using a murine stem cell virus vector with the enhanced yellow fluorescence protein (EYFP) gene (MEP). Hoxb4 transduction increased cell population in the S phase, stopped apoptosis, and recovered the impaired clonogenic, long-term culture-initiating cell (LTC-IC) and LTR activities in Rae$^{-/-}$FLC, whereas Hoxb4N>A exerted little effect (Fig. S2 *A–D* and Fig. 2*A*). Because we previously showed that accumulated Geminin gave rise to HSC deficiency in Rae$^{-/-}$FLC, we next examined the effect of Hoxb4 transduction on Geminin. Although Geminin mRNA was increased by Hoxb4 transduction as similar to mRNAs for *Cdt1* and *Cyclin A2*, target genes for E2F (Fig. S2*E*), cell sorting analysis showed that Geminin protein was significantly reduced by Hoxb4 transduction in each phase of the cell cycle (Fig. 2*B*). Down-regulation of Geminin protein was also detected in Lin$^+$, KSL, and CD34$^-$KSL subpopulations of Hoxb4-transduced BMCs (Fig. S3). Down-regulation of Geminin protein was further confirmed by immunoblot analysis in Hoxb4-transduced BMCs and 32D where the mRNA and S-phase cells were increased (Fig. 2*C* and Fig. S1 *C–F*).

Effect of Geminin on Hoxb4-Mediated Hematopoietic Induction. To examine whether down-regulation of Geminin protein is involved in the molecular mechanism underlying the Hoxb4-mediated hematopoietic induction, we examined the effect of Geminin on Hoxb4-transduced BMCs. BMCs were first transduced with Hoxb4 by using the murine stem-cell virus vector with the resistance gene for puromycin (MPI) and then were supertransduced by using the MEP vector with either Geminin or destruction box-deleted Geminin (Geminin-DBD), which is resistant to ubiquitination by the anaphase-promoting complex/cyclosome (APC/C) (26). Geminin protein was reduced by Hoxb4 transduction throughout the cell cycle, and Geminin supertransduction reverted the reduced Geminin protein level to that in control cells (Fig. 3*A*). Transduction of Geminin-DBD further up-regulated Geminin

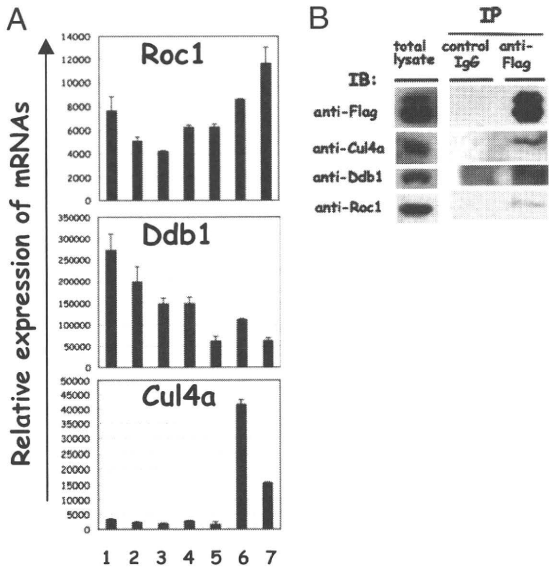

Fig. 1. Expression of Roc1, Ddb1, and Cul4a and the complex formation with Hoxb4. (*A*) mRNA expression examined by quantitative RT-PCR. The mRNA expression levels are shown as ratios to the level in GAPDH. 1, CD34$^-$KSL; 2, CD34$^+$KSL; 3, progenitors; 4, Ter119$^+$ cells (erythroid cells); 5, Gr1$^+$ cells (granulocytes); 6, CD3$^+$ cells (T cells); 7, B220$^+$ cells (B cells). (*B*) Immunoprecipitation analysis of the RDCOXB4 complex in HEK-293 transfected with Flag-Hoxb4. An anti-HA polyclonal antibody was used as a control antibody in the immunoprecipitation. IP, immunoprecipitation; IB, immunoblotting.

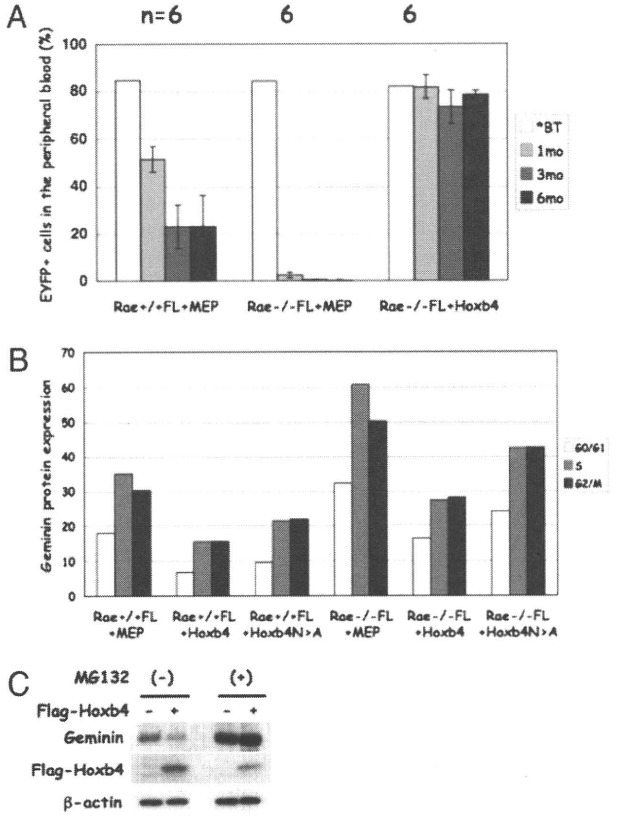

Fig. 2. Effect of Hoxb4 transduction on FLCs and BMCs. (*A*) LTR activity. Percentages of EYFP$^+$ cells in the peripheral blood cells of recipient mice were examined 1, 3, and 6 mo after transplantation. BT: before transplantation. Number of recipient mice is shown above the graph. (*B*) Geminin protein in FLCs, which were examined in each phase of the cell cycle by flow cytometry. (*C*) Geminin protein in BMCs, which were examined by immunoblot analysis. Hoxb4 transduction-mediated down-regulation of Geminin was suppressed by MG132 treatment.

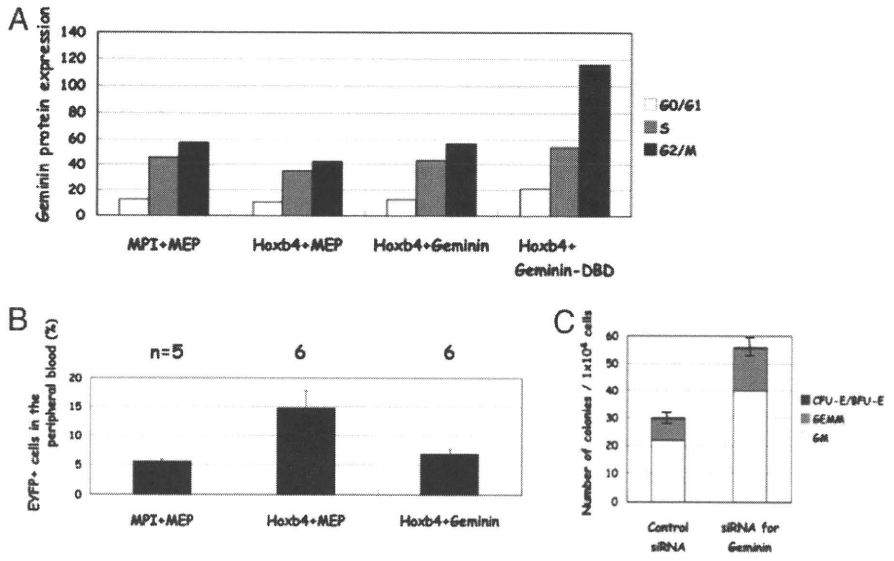

Fig. 3. Effect of Geminin transduction or knockdown in BMCs. (*A*) Effect of Geminin transduction on Geminin protein. BMCs were transduced with Hoxb4 and either Geminin or Geminin-DBD, and Geminin protein in each phase of the cell cycle was determined by flow cytometry. (*B*) Effect of Geminin transduction on LTR activity. (*C*) Effect of siRNA-induced Geminin knockdown on clonogenic activity.

protein (Fig. 3*A*). Geminin and Geminin-DBD transduction efficiently abrogated the clonogenic activity enhanced by Hoxb4 transduction (Fig. S4*A*). Geminin transduction also remarkably affected the replating, LTC-IC, and LTR activities enhanced by Hoxb4 transduction (Fig. 3*B* and Fig. S4 *B* and *C*). On the other hand, siRNA-mediated Geminin knockdown did not affect cell cycling (Fig. S5 *A* and *B*) but clearly promoted clonogenic and replating activities (Fig. 3*C* and Fig. S5 *C* and *D*). We further observed that the enhanced clonogenic activity was suppressed by restoration of Geminin (Fig. S5 *E* and *F*), confirming that the effect of the siRNA was mediated by specific down-regulation of Geminin. These findings indicated that Geminin down-regulation is crucial for Hoxb4-mediated induction of the HSC activity.

Effect of Hoxb4 on Geminin in HEK-293. We next examined the molecular mechanism of how Hoxb4 transduction down-regulated Geminin protein. Transient transfection of Hoxb4 reduced endogeneous Geminin protein in HEK-293 (Fig. 4*A*) despite increasing the mRNA (Fig. S6*A*), whereas the reduction was completely suppressed by treatment of MG132, an inhibitor of proteasome (Fig. 4*A*). Geminin down-regulation in Hoxb4-transduced BMCs and 32D was also suppressed by MG132 treatment (Fig. 2*C* and Fig. S1*F*). Pulse-chase–labeled Geminin with [^{35}S]methionine was shown to be destabilized in Hoxb4-transduced HEK-293 (Fig. S6*B*). Cul4a overexpression induced down-regulation of Geminin protein synergistically with Hoxb4 (Fig. S6*C*). siRNA-mediated knockdown of Cul4a eliminated the downregulating effect of Hoxb4 on Geminin protein (Fig. 4*B*), which facilitated our examination of the involvement of Cul4a in Hoxb4-mediated Geminin regulation. Mobility-shifted Geminin bands were detected in extracts from HEK-293 cotransfected with Geminin, hemagglutinin (HA)-tagged ubiquitin (HA-Ub), and Hoxb4 or Cul4a in the presence of MG132 (Fig. S7*A*). Mobility-shifted Geminin bands were confirmed to be ubiquitin-conjugated Geminin by means of immunoprecipitation analysis (Fig. S7*B*). Ubiquitination of Geminin-DBD through Hoxb4 was similar to that of Geminin (Fig. S7*A*), suggesting that the Hoxb4-mediated ubiquitination was independent of APC/C. The above-mentioned findings support a hypothesis that transduced Hoxb4 down-regulates Geminin protein through the ubiquitin-proteasome system (UPS) with the RDCOXB4 complex as the E3 ubiquitin ligase.

Reconstitution of E3 Ubiquitin Ligase Activity of RDCOXB4 for Geminin. To determine the E3 ubiquitin ligase activity of the RDCOXB4 complex for Geminin, we reconstituted the recombinant protein complex in *Spodoptera frugiperda* insect cells, named Sf9. Sf9 were coinfected with baculoviruses including His6-Roc1, Ddb1, Cul4a (27), and Flag-Hoxb4. Cell extracts were then prepared from Sf9-expressing (His6-Roc1)-Ddb1-Cul4a-(Flag-Hoxb4)[RDCOXB4], which was purified with metal affinity column chromatography. Gel filtration fractionation analysis showed that one of the peak fractions of Flag-Hoxb4 corresponded with the complex with a molecular weight similar to that of the recombinant complex consisting of stoichiometrically determined amounts of the components (260 kDa) (Fig. S8*A*). We also prepared and purified (GST-Roc1)-Ddb1-Cul4a-(Flag-Hoxb4) [RDCOXB4] with glutathione affinity column chromatography (Fig. 5*A*). The affinity-purified recombinant

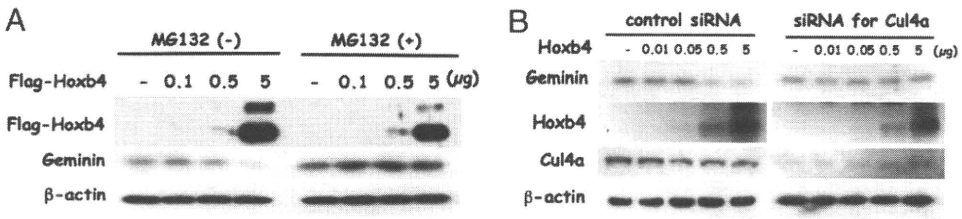

Fig. 4. Effect of Hoxb4 or Cul4a on Geminin protein in HEK-293. (*A*) Effect of Hoxb4 transfection on Geminin protein, which was examined by immunoblot analysis. The effect was suppressed by MG132 treatment. (*B*) Effect of Cul4a knockdown on Hoxb4-mediated down-regulation of Geminin protein.

RDCOXB4 was then subjected to an in vitro ubiquitination assay with purified bacterially produced recombinant His6- and myc-tagged Geminin (myc-Geminin). Mobility-shifted Geminin bands were detected in the reaction products (Fig. S8*B*). Intensity of the bands increased and mobility also shifted according to dosage of the RDCOXB4 complex and the reaction time. Next, an in vitro ubiquitination assay with biotin-tagged ubiquitin (biotin-ubiquitin) was performed to determine whether the shifted bands corresponded with ubiquitinated Geminin (Fig. 5*B*). myc-Geminin was then immunoprecipitated with an anti-myc polyclonal antibody after the reaction, and similar mobility-shifted bands were detected in the immunoprecipitate through biotin–avidin interaction, confirming that the mobility-shifted bands represented ubiquitinated Geminin. The lower two mobility-shifted bands (Fig. S8*C*) were detectable in the reaction products obtained with methyl-ubiquitin, whereas more mobility-shifted bands were not, indicating that the former corresponded to mono-ubiquitinated Geminin and the latter to Geminin with more elongated ubiquitin chains.

Hoxb4N>A tended to form the RDCOXB4 complex more efficiently and/or stably than did wild-type Hoxb4 (Fig. 5*A*). The poly-ubiquitination activity was, however, abrogated by a single amino acid substitution (Fig. 5*C*), suggesting that the E3 ubiquitin ligase activity for Geminin of RDCOXB4 was mediated by a homeodomain in Hoxb4, which provides an interaction domain with Geminin. These findings clearly showed in vitro that Hoxb4 formed the RDCOXB4 complex and acted as the E3 ubiquitin ligase for Geminin. We also compared E3 ubiquitin ligase activities in GST-Roc1, RDOXB4(-Cul4a), RDC(-Hoxb4), RCOXB4 (-Ddb1), and RDCOXB4 (Fig. 5 *A* and *C*). The mobility-shifted bands for poly-ubiquitinated Geminin were undetectable in GST-Roc1, RDOXB4(-Cul4a), RDC(-Hoxb4), and RCOXB4(-Ddb1) although those for mono-ubiquitinated Geminin were detectable (Fig. 5*C*). Even in the absence of either Cul4a or Ddb1, GST-Roc1 interacted with Hoxb4 but displayed mono-ubiquitination activity only for Geminin (Fig. 5*C*). Each of the RDCOXB4 members may thus be required for an effective induction of poly-ubiquitination. To eliminate the possibility that Geminin was ubiquitinated by contaminated APC/C, we confirmed that a similar activity occurred in Geminin-DBD (Fig. S8*D*). We also examined ubiquitination of each of the RDCOXB4 members in the reaction products. The RDCOXB4 complex itself may thus also be subjected to self-ubiquitination (Fig. S8*E*).

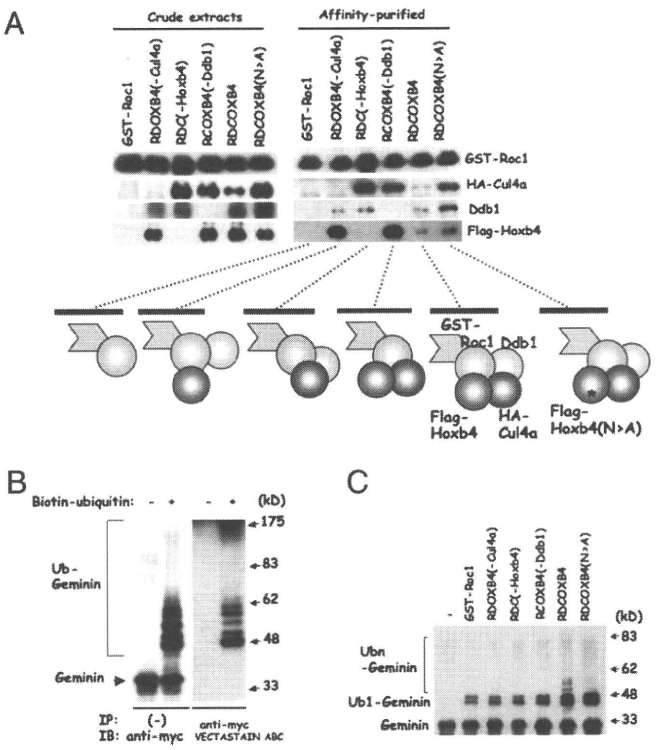

Fig. 5. Reconstitution and purification of the RDCOXB4 complex in Sf9 and E3 ubiquitin ligase activity for Geminin. (*A*) Crude extracts: expression of each member of the complex was detected in crude extracts by immunoblot analysis. Affinity-purified: pull-down assay of the complex with GST-Roc1. (*Lower*) Schematic representation of the complex. *, N>A mutation in the homeodomain of Hoxb4. (*B* and *C*) E3 ubiquitin ligase activity for Geminin. The affinity-purified recombinant complex was subjected to in vitro ubiquitination reaction (myc-Geminin + E1 + E2 + ubiquitin). (*B*) Reaction with biotin-tagged ubiquitin. Ubiquitinated Geminin was detected through biotin–avidin interaction in immunoprecipitated myc-Geminin. (*C*) The E3 ubiquitin ligase activity for Geminin in GST-Roc1, RDOXB4(-Cul4a), RDC(-Hoxb4), RCOXB4(-Ddb1), RDCOXB4, and RDCOXB4 (N>A). The amount of GST-Roc1 in the complex was adjusted to that of RDCOXB4 (1 μg).

Effect of Hoxb4 Transduction on E2F Activity and Its Target Gene Expression. Hoxb4 transduction increased mRNA for *Geminin*, *Cdt1*, and *Cyclin A2* in either $Rae^{+/+}$FLC or $Rae^{-/-}$FLC, whereas Hoxb4N>A did so less efficiently (Fig. S2*E*). Because these genes are under the regulation of E2F (28, 29), the induction was presumed to be mediated by E2F activation. We next examined the effect of Hoxb4 on E2F activity by means of a transient transfection experiment with an E2F-firefly luciferase reporter plasmid, pE2WTx4-Luc, in HEK-293 (Fig. 6*A*) (30). Hoxb4 overexpression induced luciferase activity in a dosage-dependent manner, but that of Hoxb4N>A did so less efficiently (Fig. 6*A*). Because Hoxb4 transfection reduced Geminin protein through UPS as mentioned above, we examined the effect of Geminin on E2F activity (Fig. 6*A*). siRNA-mediated knockdown of Geminin-induced E2F activity and restoration of reduced Geminin by 6myc-tagged Geminin transfection significantly reversed the effect, suggesting that Hoxb4 induced E2F activity at least in part through the direct regulation of Geminin.

Effect of Hoxb4 Transduction on Cdt1 and Mcm2. Finally, we examined by immunoblot analysis the effect of Hoxb4 on Cdt1 in the whole extract (Fig. S2*F*) as well as in the chromatin fraction (Fig. 6*B*). Transduction of Hoxb4 increased Cdt1 in the whole extract (Fig. S2*F*), probably through the aforementioned E2F activation, whereas that of Hoxb4N>A increased less efficiently. Similar induction was observed in Cyclin A2 (Fig. S2*F*) and Mcm2 (Fig. 6*B*). Hoxb4 transduction more prominently increased Cdt1 and Mcm2 in the chromatin fraction of $Rae^{-/-}$FLC (Fig. 6*B*), in which chromatin-loaded Cdt1 and Mcm2 were markedly reduced by accumulated Geminin as described previously (20). The down-regulation of Geminin protein was thus presumed to increase chromatin-loaded Cdt1 and Mcm2 either by E2F activation or by relieving the Geminin-mediated direct inhibition of Cdt1, promoting the prereplicative complex formation on chromatin to provide cells with higher proliferation potential.

Discussion

We show here that Hoxb4 directly interacts with Geminin through the homeodomain. Hoxb4 transduction induced formation of the RDCOXB4 complex, which may act as the E3 ubiquitin ligase for Geminin, whereas Hoxb4N>A constituted a similar complex that displayed little of the E3 ubiquitin ligase activity. Although the homeodomain of Hox proteins has long been believed to function as a DNA-binding domain (7), these findings indicate that the homeodomain may provide the RDCOXB4 complex with a recognition domain for Geminin. The involvement of the Roc1-Ddb1-Cul4a ubiquitin ligase core component in sustaining HSC activity is further supported by recently reported

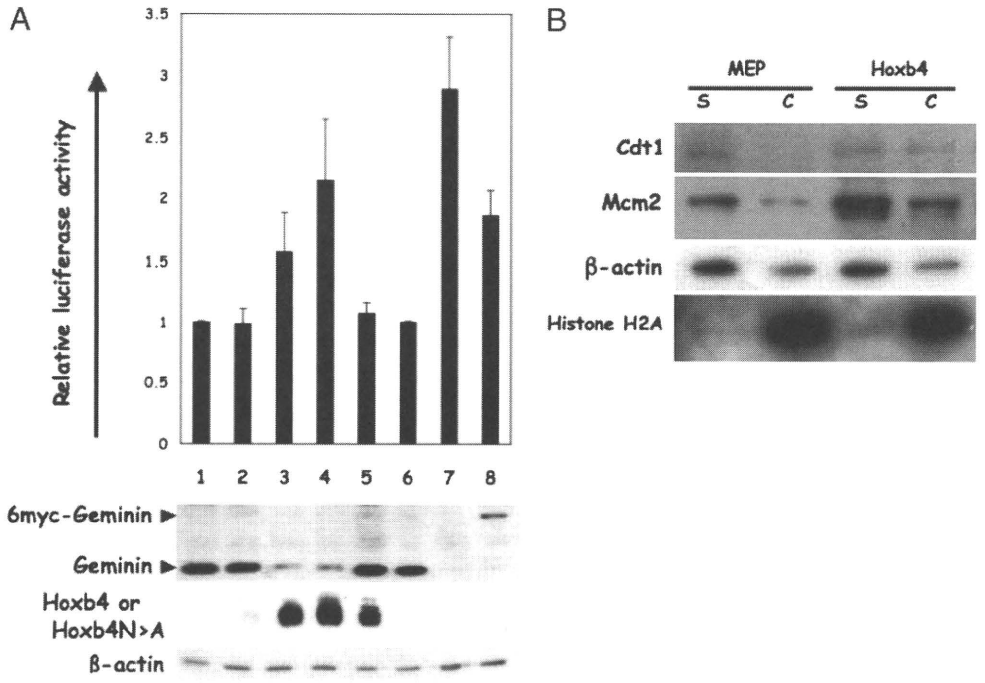

Fig. 6. Effect of Hoxb4 on E2F activity and DNA replication licensing. (*A*) Effect of Hoxb4 transfection on E2F activity. Renilla luciferase reporter plasmid driven by the mutant E2F-binding site, pE2MTx4-R, was used as control. (*Upper*) Firefly luciferase activity relative to that in mock vector-transfected cells. 1, mock vector; 2, Hoxb4—0.1 μg; 3, Hoxb4—0.5 μg; 4, Hoxb4—1 μg; 5, Hoxb4N>A—1 μg; 6, control siRNA; 7, siRNA for Geminin and a mock vector; 8, siRNA for Geminin and 6myc-tagged Geminin (0.1 μg). (*Lower*) Immunoblot analysis. (*B*) Effect of Hoxb4 transduction on Cdt1 and Mcm2 in the chromatin fraction of $Rae^{-/-}$FLC. S, soluble fraction; C, chromatin fraction. β-Actin and histone H2A were detected as control to ensure equal amounts of protein and purity of the chromatin fraction, respectively.

genetic evidence that the self-renewal and repopulating capacities, as well as hematopoietic differentiation, were impaired by *Cul4a* haploinsufficiency (24), although many target molecules for the Roc1-Ddb1-Cul4a component were reported. Hoxb4 transduction may down-regulate Geminin protein through UPS to relieve the inhibition of Cdt1, and down-regulated Geminin protein may also give rise to E2F activation, which facilitates loading of a DNA prereplicative complex onto chromatin to promote cell cycling. Because E2F activity was reported to be induced by Hoxb4 through the induction of c-Myc as mentioned above (9), Hoxb4 might induce E2F activity through either down-regulation of Geminin or up-regulation of c-Myc. Although it remains elusive in our study how down-regulated Geminin induces the E2F activation, the above findings suggest that Geminin by itself negatively regulates the transcription activity of its own promoter because transcription of *Geminin* is under the regulation of E2F (29). This may imply that a feedback mechanism plays a role in maintaining homeostasis of Geminin expression in cells. Hoxb4 transduction may thus affect Geminin homeostasis directly and indirectly, i.e., via the ubiquitination of Geminin and also via its effect on the transcription of *Geminin* to induce the HSC activity.

Although further detailed analysis is required, we propose a tentative model for the molecular mechanism showing how transduced Hoxb4 provides hematopoietic stem and progenitor cells with high proliferation potential on the basis of the findings in our current study (Fig. 7). Transduced Hoxb4 induces UPS-mediated down-regulation of Geminin protein by constituting the RDCOXB4 complex, an E3 ubiquitin ligase for Geminin, which results in augmentation of a prereplicative complex loaded onto chromatin as well as in transcription induction of the E2F target genes involved in DNA replication and cell cycling. The augmented prereplicative complex loaded onto chromatin may provide higher proliferation potential for hematopoietic stem and progenitor cells. As we previously reported, Geminin is highly expressed in $CD34^{-}KSL$ but is down-regulated in $CD34^{+}KSL$, progenitors, and their progeny subpopulations, whereas Cdt1 expression is reciprocal to Geminin expression (20). Thus, high Geminin expression is presumed to induce $CD34^{-}KSL$ to maintain quiescence and undifferentiated states through direct interaction with Cdt1(19) and Brg1/Brahma (21), respectively, whereas down-regulated Geminin may induce cellular proliferation and differentiation in the progeny subpopulations. Although the higher cellular proliferation potential might also help to induce self-renewal of HSCs, the precise molecular role for Geminin in Hoxb4 transduction-induced self-renewal activation of HSCs remains in-

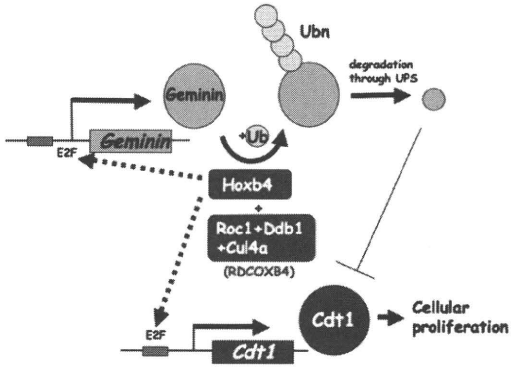

Fig. 7. Proposed tentative model for the molecular role of Hoxb4 in providing cells with proliferation potential. The pathway either enhanced or diminished by Hoxb4 transduction is indicated by thick and thin lines, respectively. Dotted lines indicated an indirect effect. E2F, E2F-binding site; Ub, ubiquitin.

sufficiently understood. Further detailed analysis of Geminin could provide an important clue for elucidating a molecular mechanism that sustains the hematopoietic stem and progenitor cell activity.

Materials and Methods

Animal experiments were done with C57BL6 mice and mice deficient in *Rae28* with a congenic genetic background. Plasmids and double-stranded RNAs (Dharmacon-ThermoFisher) were transfected by the calcium phosphate coprecipitation method and by using Lipofectamine RNAiMAX (Invitrogen-Life Technologies). Retrovirus-mediated gene transduction was performed with murine stem cell virus vectors. Hematopoiesis was assessed through clonogenic, LTC-IC, and LTR activities. The recombinant RDCOXB4 complexes were purified from Sf9 transfected with the baculovirus vectors and subjected to the in vitro ubiquitination assay. The statistically analyzed results are shown with SEM. A detailed description of all of the methods and antibodies used appear in *SI Materials and Methods* and in Table S1, respectively.

ACKNOWLEDGMENTS. We thank Drs. R. K. Humphries (University of British Columbia, Vancouver) and M. Kyba (University of Minnesota, Minneapolis) for providing the Hoxb4 cDNA; Dr. A. Kikuchi (Osaka University, Suita) for providing the pV-IKS and pVL1392 vectors; Dr. T. Inaba (Hiroshima University, Hiroshima) for the 32D cell line; the Analysis Center of Life Science in Hiroshima University, Ms. R. Tokimoto, and Y. Nakashima for technical assistance; Dr. M. Kanno (Hiroshima University, Hiroshima) for supporting Y.O., and Ms. A. Harada and H. Shimamoto for secretarial assistance. This work was supported by Grants-in-Aid for Scientific Research from the Ministry of Education, Culture, Sports, Science and Technology of Japan and by the Uehara Memorial Foundation, the Yamanouchi Foundation for Research on Metabolic Disorders, the Japan Leukaemia Research Fund, the Mitsubishi Pharma Research Foundation, the Novartis Foundation for the Promotion of Science, the Daiwa Securities Health Foundation, and the UBE Foundation.

1. Sauvageau G, et al. (1995) Overexpression of *HOXB4* in hematopoietic cells causes the selective expansion of more primitive populations in vitro and in vivo. *Genes Dev* 9: 1753–1765.
2. Antonchuk J, Sauvageau G, Humphries RK (2002) HOXB4-induced expansion of adult hematopoietic stem cells ex vivo. *Cell* 109:39–45.
3. Buske C, et al. (2002) Deregulated expression of HOXB4 enhances the primitive growth activity of human hematopoietic cells. *Blood* 100:862–868.
4. Kyba M, Perlingeiro RC, Daley GQ (2002) HoxB4 confers definitive lymphoid-myeloid engraftment potential on embryonic stem cell and yolk sac hematopoietic progenitors. *Cell* 109:29–37.
5. Amsellem S, et al. (2003) Ex vivo expansion of human hematopoietic stem cells by direct delivery of the HOXB4 homeoprotein. *Nat Med* 9:1423–1427.
6. Krosl J, et al. (2003) In vitro expansion of hematopoietic stem cells by recombinant TAT-HOXB4 protein. *Nat Med* 9:1428–1432.
7. McGinnis W, Krumlauf R (1992) Homeobox genes and axial patterning. *Cell* 68: 283–302.
8. Beslu N, et al. (2004) Molecular interactions involved in HOXB4-induced activation of HSC self-renewal. *Blood* 104:2307–2314.
9. Satoh Y, et al. (2004) Roles for c-Myc in self-renewal of hematopoietic stem cells. *J Biol Chem* 279:24986–24993.
10. Schiedlmeier B, et al. (2007) HOXB4's road map to stem cell expansion. *Proc Natl Acad Sci USA* 104:16952–16957.
11. Ohta H, et al. (2002) Polycomb group gene rae28 is required for sustaining activity of hematopoietic stem cells. *J Exp Med* 195:759–770.
12. Park IK, et al. (2003) Bmi-1 is required for maintenance of adult self-renewing haematopoietic stem cells. *Nature* 423:302–305.
13. Wang H, et al. (2004) Role of histone H2A ubiquitination in Polycomb silencing. *Nature* 431:873–878.
14. Takihara Y, et al. (1997) Targeted disruption of the mouse homologue of the *Drosophila polyhomeotic* gene leads to altered anteroposterior patterning and neural crest defects. *Development* 124:3673–3682.
15. Bracken AP, et al. (2007) The Polycomb group proteins bind throughout the INK4A-ARF locus and are disassociated in senescent cells. *Genes Dev* 21:525–530.
16. Chagraoui J, et al. (2006) E4F1: A novel candidate factor for mediating BMI1 function in primitive hematopoietic cells. *Genes Dev* 20:2110–2120.
17. Pomerantz J, et al. (1998) The Ink4a tumor suppressor gene product, p19Arf, interacts with MDM2 and neutralizes MDM2's inhibition of p53. *Cell* 92:713–723.
18. Le Cam L, et al. (2006) E4F1 is an atypical ubiquitin ligase that modulates p53 effector functions independently of degradation. *Cell* 127:775–788.
19. Blow JJ, Hodgson B (2002) Replication licensing: Defining the proliferative state? *Trends Cell Biol* 12:72–78.
20. Ohtsubo M, et al. (2008) Polycomb-group complex 1 acts as an E3 ubiquitin ligase for Geminin to sustain hematopoietic stem cell activity. *Proc Natl Acad Sci USA* 105: 10396–10401.
21. Seo S, et al. (2005) Geminin regulates neuronal differentiation by antagonizing Brg1 activity. *Genes Dev* 19:1723–1734.
22. Luo L, Yang X, Takihara Y, Knoetgen H, Kessel M (2004) The cell-cycle regulator geminin inhibits Hox function through direct and polycomb-mediated interactions. *Nature* 427:749–753.
23. Kim MY, et al. (2006) A repressor complex, AP4 transcription factor and geminin, negatively regulates expression of target genes in nonneuronal cells. *Proc Natl Acad Sci USA* 103:13074–13079.
24. Li B, et al. (2007) Cul4A is required for hematopoietic stem-cell engraftment and self-renewal. *Blood* 110:2704–2707.
25. Zhang Y, et al. (2003) CUL-4A stimulates ubiquitylation and degradation of the HOXA9 homeodomain protein. *EMBO J* 22:6057–6067.
26. McGarry TJ, Kirschner MW (1998) Geminin, an inhibitor of DNA replication, is degraded during mitosis. *Cell* 93:1043–1053.
27. Ohta T, Michel JJ, Schottelius AJ, Xiong Y (1999) ROC1, a homolog of APC11, represents a family of cullin partners with an associated ubiquitin ligase activity. *Mol Cell* 3:535–541.
28. Schulze A, et al. (1995) Cell cycle regulation of the cyclin A gene promoter is mediated by a variant E2F site. *Proc Natl Acad Sci USA* 92:11264–11268.
29. Yoshida K, Inoue I (2004) Regulation of Geminin and Cdt1 expression by E2F transcription factors. *Oncogene* 23:3802–3812.
30. Ohtani K, et al. (2000) Cell type-specific E2F activation and cell cycle progression induced by the oncogene product Tax of human T-cell leukemia virus type I. *J Biol Chem* 275:11154–11163.

Hum Genet (2010) 127:619–628
DOI 10.1007/s00439-010-0822-7

REVIEW ARTICLE

Molecular pathogenesis of a novel mutation, G108D, in short-chain acyl-CoA dehydrogenase identified in subjects with short-chain acyl-CoA dehydrogenase deficiency

Kenichiro Shirao · Satoshi Okada · Go Tajima · Miyuki Tsumura · Keiichi Hara · Shin'ichiro Yasunaga · Motoaki Ohtsubo · Ikue Hata · Nobuo Sakura · Yosuke Shigematsu · Yoshihiro Takihara · Masao Kobayashi

Received: 22 February 2010 / Accepted: 30 March 2010 / Published online: 8 April 2010

Abstract Short-chain acyl-CoA dehydrogenase (SCAD) is a mitochondrial enzyme involved in the β-oxidation of fatty acids. Genetic defect of SCAD was documented to cause clinical symptoms such as progressive psychomotor retardation, muscle hypotonia, and myopathy in early reports. However, clinical significance of SCAD deficiency (SCADD) has been getting ambiguous, for some variants in the *ACADS* gene, which encodes the SCAD protein, has turned out to be widely prevailed among general populations. Accordingly, the pathophysiology of SCADD has not been clarified thus far. The present report focuses on two suspected cases of SCADD detected through the screening of newborns by tandem mass spectrometry. In both subjects, compound heterozygous mutations in *ACADS* were detected. The mutated genes were expressed in a transient gene expression system, and the enzymatic activities of the obtained mutant SCAD proteins were measured. The activities of the mutant SCAD proteins were significantly lower than that of the wild-type enzyme, confirming the mechanism underlying the diagnosis of SCADD in both subjects. Moreover, the mutant SCAD proteins gave rise to mitochondrial fragmentation and autophagy, both of which were proportional to the decrease in SCAD activities. The association of autophagy with programed cell death suggests that the mutant SCAD proteins are toxic to mitochondria and to the cells in which they are expressed. The expression of recombinant *ACADS*-encoded mutant proteins offers a technique to evaluate both the nature of the defective SCAD proteins and their toxicity. Moreover, our results provide insight into possible molecular pathophysiology of SCADD.

K. Shirao and S. Okada contributed equally to this work.

Nucleotide sequence data reported are available in the DDBJ database under the accession number AB527081.

Electronic supplementary material The online version of this article (doi:10.1007/s00439-010-0822-7) contains supplementary material, which is available to authorized users.

K. Shirao · S. Okada · G. Tajima (✉) · M. Tsumura · K. Hara · M. Kobayashi
Department of Pediatrics, Hiroshima University Graduate School of Biomedical Sciences, 1-2-3 Kasumi, Minami-ku, Hiroshima 734-8551, Japan
e-mail: acadugo@mac.com

S. Yasunaga · M. Ohtsubo · Y. Takihara
Department of Stem Cell Biology, Research Institute for Radiation Biology and Medicine, Hiroshima University, Hiroshima 734-8553, Japan

I. Hata
Department of Pediatrics, Faculty of Medical Sciences, University of Fukui, Fukui 910-1193, Japan

N. Sakura
Nursing House for Severe Motor and Intellectual Disabilities "Suzugamine", Hiroshima 731-5122, Japan

Y. Shigematsu
Department of Health Science, Faculty of Medical Sciences, University of Fukui, Fukui 910-1193, Japan

Introduction

Short-chain acyl-CoA dehydrogenase (SCAD), a mitochondrial enzyme of the fatty acid β-oxidation system, mediates the metabolic transition from acyl-CoA with four- or six-carbon chains to 2-enoyl-CoA in the first step of the β-oxidation spiral. SCAD deficiency (SCADD) occurs as a rare autosomal recessive disorder, first reported in 1985 (Amendt et al. 1987; Bennett et al. 1985; Coates et al.

1988). The clinical symptoms such as progressive psychomotor retardation, muscle hypotonia, and myopathy were documented (Bhala et al. 1995; Corydon et al. 2001). As the results of the enzymatic defects, increased levels of C_4-acylcarnitine in peripheral blood and ethylmalonic acid (EMA) in urine are observed.

Acylcarnitine measurement using tandem mass spectrometry (MS/MS) is a new screening technology that has been applied to the detection of inborn errors of organic acid and fatty acid metabolism in newborns, including those with symptomatic and asymptomatic SCADD as well as their asymptomatic siblings (Bok et al. 2003; Naito et al. 1989b; Pedersen et al. 2008). This has led to the recognition that in the general population, many individuals may carry *ACADS* mutations but lack SCADD-related symptoms. Precise knowledge of the pathogenesis, natural course, and prognosis of SCADD, based on a definitive diagnosis, is essential for promoting a better understanding about SCADD and for developing an even more efficient screening system.

Mutations in the *ACADS* gene, which encodes the SCAD protein, have been identified in symptomatic patients with SCADD. Overall, approximately 60 mutations in *ACADS* are known thus far (Gregersen et al. 2008). These may result in an insufficient energy supply during β-oxidation, especially under conditions of starvation or stress, thereby triggering the onset of SCADD (Gregersen et al. 2001). Indeed, two studies reported a correlation between *ACADS* mutations and the deterioration of SCAD enzymatic activities (Naito et al. 1989a, b). However, the residual enzymatic activities documented in those studies were, in many patients, too high to allow a definitive diagnosis of SCADD although this may have been due to the overlapping activity of MCAD toward C4–C6 acyl-CoAs (Wanders et al. 1999).

Two common *ACADS* sequence variants, R171W (511C>T) and G209S (625G>A), have been identified in healthy populations at a frequency of 14–30% (Corydon et al. 1996, 2001; Gregersen et al. 1998; Pedersen et al. 2008). Genetic analysis of patients with elevated levels of ethylmalonate in the urine revealed that approximately 69% was homozygous or compound heterozygous for these variants (Gregersen et al. 2001). Although neither of the variants seems to be sufficient to cause disease, it cannot be ruled out that expression of either one may nonetheless contribute to disease pathogenesis in conjunction with other, hitherto unknown factors (van Maldegem et al. 2006). Thus, whether mutations in *ACADS* are related directly to the deterioration of short-chain fatty acid oxidation and to the clinical symptoms of SCADD remain controversial.

In this study, we identified the first two cases of SCADD in Japan, including one subject with a novel *ACADS* G108D mutation. Analysis of the recombinant SCAD mutant proteins showed that all of them give rise to a severe decrease in SCAD enzymatic activity. Furthermore, differences in the solubility, degree of mitochondrial fragmentation, and autophagy were identified among SCAD wild-type (WT), mutant, and variant proteins. Together with recent studies in which a correlation between mitochondrial fragmentation and neurodegeneration was demonstrated (Knott et al. 2008), our findings may provide an important clue regarding the molecular mechanism underlying SCADD and the neuronal symptoms possibly associated with the disease.

Materials and methods

Case report

Newborns with metabolic disorders of organic and fatty acids have been screened in Hiroshima using MS/MS technology since 1999. Based on the screening results, two females suspected of having SCADD were identified from among the more than 200,000 infants screened. In these two subjects, high levels of C_4-acylcarnitine were detected in blood spotting by MS/MS, and the level of ethylmalonic acid excreted in urine was elevated as well (Sup. Table 1). According to these criteria, the subjects were susceptible to SCADD; however, the children, who are now 4-year-old, have thus far not shown any symptom related to SCADD, and neither do the members of their families.

Blood samples were obtained from the subjects and from healthy adult controls after they provided written informed consent. The study was approved by the Ethics Committee/Internal Review Board of Hiroshima University.

Molecular genetics

Genomic DNA was extracted from peripheral white blood cells. All of the exons and flanking introns comprising the *ACADS* gene were PCR-amplified using the primers listed in Sup. Table 2. The PCR products were sequenced directly using a BigDye Terminator v3.1 cycle sequencing kit (Applied Biosystems, Foster City, CA, USA) and an ABI PRISM 310 genetic analyzer (Applied Biosystems).

Total RNA was extracted from the cells using ISOGEN (Nippon Gene Co., Tokyo, Japan), and the cDNA was synthesized from 5 μg of total RNA using a SuperScript first-strand synthesis system for RT-PCR (Invitrogen, Carlsbad, CA, USA). PCR of the WT and mutant alleles was carried out with primers that spanned the entire *ACADS* coding region. The PCR products were cloned into pGEM-T Easy vector (Promega, Madison, WI, USA). The three mutants were generated by PCR-based mutagenesis of the WT construct using the mismatched PCR primers listed in

Sup. Table 2. These fragments were subcloned into the *Eco*RI and *Xho*I sites of the mammalian expression vector PcDNA myc-His (+) (Invitrogen).

Analysis of gene expression

The SCAD dehydrogenase activity targeting C4-CoA is maximal in the mitochondrial fatty acid cycle, but similar enzymatic activity, at comparable levels, is expressed by MCAD in a reaction involving the same substrate (Coates et al. 1988; Wanders et al. 1999). Thus, in studies examining SCAD enzymatic activities, MCAD enzymatic activity was neutralized by pre-treating fibroblasts, lymphocytes, and muscle samples with a polyclonal antibody against the latter protein; nonetheless, SCAD enzymatic activities varied greatly (Corydon et al. 1997; 2001; Gregersen et al. 1998; Naito et al. 1989b; Tein et al. 2008). Therefore, it is unclear whether the in vitro data obtained in those studies of SCADD patients reflected only SCAD, and not MCAD, activity. Initially, we also tried to measure cellular SCAD enzymatic activity by pre-treating the cells with a polyclonal antibody against MCAD, but, likewise, the data were not convincing. Therefore, we devised a transient gene expression system that overcame the contaminating influence of MCAD.

HEK293 cells were maintained in DMEM containing 10% fetal calf serum (FCS) (HyClone, Logan, UT, USA), 100 U penicillin/ml, and 100 μg streptomycin/ml. At 24 h before transfection, the cells were harvested by trypsinization and replated at a density of 1×10^6 cells/ml in 100-mm culture dishes. Plasmid DNA (5 μg per plate) carrying the WT, P55L, G108D, E344G, R171W, or G209S alleles of *ACADS* was introduced into HEK293 cells by calcium phosphate-mediated transfection.

Enzymatic activity assays were carried out at 24 h post-transfection using 2×10^5 cells from each plate and following a previously reported method, with some modification (Tajima et al. 2005). In brief, the reaction mixture contained 80 mM K_2HPO_4 (pH 7.0), 1 mM *n*-butyryl-CoA (Sigma Chemical, St. Louis, MO, USA), 2 mM phenazine methosulfate (Nacalai Tesque, Tokyo, Japan), 0.1 mM flavin adenine dinucleotide, and the cell lysate. After incubation at 37°C for 5 min, the reactions were terminated by the addition of 0.3 mM $HClO_4$. The denatured proteins were centrifuged, and the supernatant introduced into a high-performance liquid chromatography (HPLC) system set up to detect crotonyl-CoA production based on its UV absorption at 260 nm. A linear increase of crotonyl-CoA production was detected within the range of 0.5×10^5–3.0×10^5 HEK293 cells; thus, in subsequent experiments, extracts were prepared from 2×10^5 HEK293 cells. The same assays were carried out at 26 and 41°C incubation temperatures.

The remainder of the cell extracts was used for Western blotting, in which the SCAD protein was detected using anti-Myc antibodies.

Separation of the SCAD proteins into soluble and insoluble fractions

Plasmids carrying the WT, P55L, G108D, E344G, R171W, or G209S *ACADS* alleles were introduced into HEK293 cells by calcium phosphate-mediated transfection. At 24 h post-transfection, 5×10^5 cells from each plate were transferred to 1.5-ml Eppendorf tubes and washed with 1× PBS. The cells were treated with extraction buffer (10% glycerol, 0.15 mM KCl, 1.5 mM MgCl2, 1 mM EDTA, 0.5% Triton X-100, 20 mM HEPES, with protease inhibitor), vortexed, and then set on ice for 10 min, followed by centrifugation (17,000×*g*, 10 min, 4°C) to isolate the soluble and insoluble fractions. Since SCAD mutant proteins have a tendency to misfold and aggregate, they are predominately contained in the insoluble fraction (Pedersen et al. 2003). WT proteins and proteins encoded by the common variants are found almost in the soluble fraction. Accordingly, both the supernatants, as the soluble fraction, and the pellets, as the insoluble fraction, were analyzed by Western blotting.

Immunostaining of the SCAD proteins

The U2-OS cells were maintained in DMEM containing 10% fetal calf serum (FCS) (HyClone, Logan, Utah, USA), 100 U penicillin/ml, and 100 μg streptomycin/ml. At 24 h before transfection, the cells were harvested by trypsinization and replated at a density of 2×10^5 cells/ml in 35-mm culture dishes with a cover glass. Plasmid DNA (1 μg per plate) carrying the WT, P55L, G108D, E344G, R171W, or G209S *ACADS* alleles were introduced into U2-OS cells by lipofection using lipofectamine 2000 according to the manufacturer's guidelines (Invitrogen). The cells were stained 24 h post-transfection with an anti-c-Myc rabbit polyclonal IgG (200 μg/ml; Santa Cruz Biotechnology) and an Alexa Fluor 488 goat anti-rabbit IgG (2 mg/ml; Molecular Probes) for SCAD proteins, Hoechst 33342 1 μg/ml (Calbiochem) for nuclei, and MitoTracker Red CM-H_2XRos (Molecular Probes) for mitochondria. Images were taken using an OLYMPUS microscope BX50 equipped with DP70. Stained cells were photographed at the same exposure time for each dye to allow comparison.

Mitochondrial fragmentation data were evaluated statistically and expressed as the means and SE. Experiments were performed in triplicate and repeated at least three times. Statistical analysis was carried out using Student's *t* tests; $^{**}p < 0.01$; $^{***}p < 0.001$.

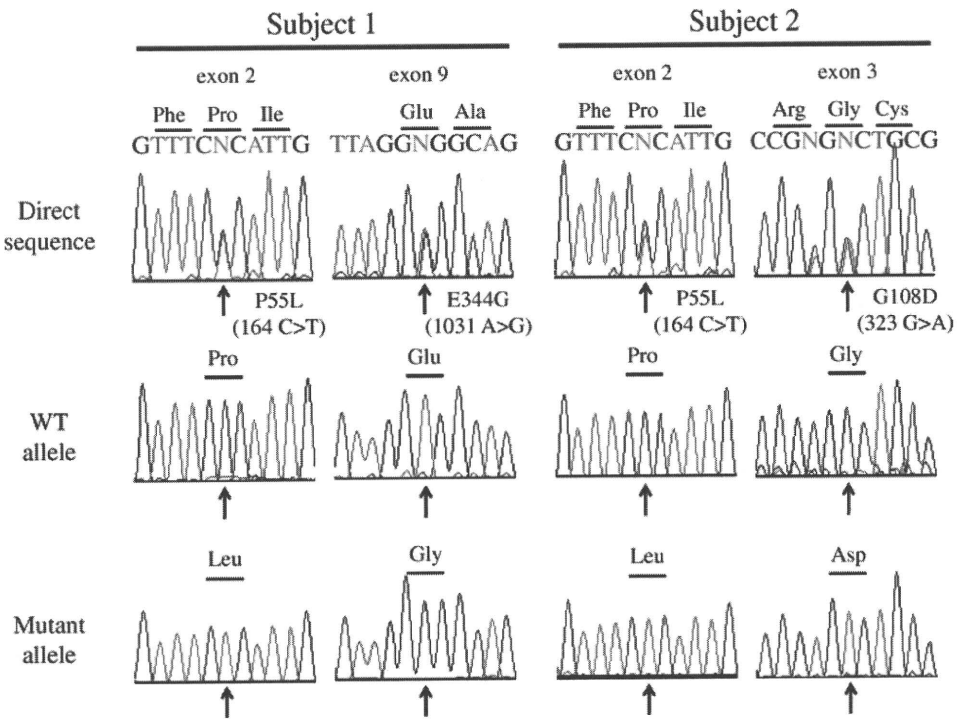

Fig. 1 Sequence analysis of *ACADS*. Genomic DNAs of *ACADS* from the two subjects who positively screened for SCADD were amplified by PCR, and the products were sequenced by direct sequencing. Sequencing analysis revealed compound heterozygous *ACADS* mutations in both subjects. *Upper row* shows each of sequence of the mutations; Subject 1: Pro55Leu (164C>T) in exon 2 and Glu344Gly (1031A>G) in exon 9; subject 2: Pro55Leu (164C>T) in exon 2 and Gly108Asp (323G>A) in exon 3. *Middle row* showed WT allele sequences of *ACADS*, and *lower row* showed each mutant allele of the subjects

Autophagy analysis of the SCAD-overexpressing cells

The autophagic activities of cells overexpressing WT or G108D mutant SCAD proteins were analyzed in whole-cell lysates prepared as follows: 1×10^6 U2-OS cells were transfected with 5 μg WT or G108D plasmid DNAs by lipofection. At 24 and 48 h post-transfection, the cells were collected and treated with 2× SDS-PAGE buffer. The resulting lysates of these WT and G108D SCAD-overexpressing cells were analyzed by Western blotting using a polyclonal anti-LC3B antibody (1 mg/ml; NOVUS Biologicals) in order to detect LC3-II expression which is induced by autophagosome formation. As a control, whole-cell lysates were prepared from 1×10^6 U2-OS cells with and without pepstatinA and E64d, both of which inhibit the conversion of LC3-II to LC3-I.

Results

Sequence analysis

High molecular weight DNA was extracted from peripheral blood samples obtained from the two subjects diagnosed with SCADD. Exons and the flanking intron regions of *ACADS* were amplified by PCR (Fig. 1). As shown in Fig. 1, both subjects had missense mutations in the *ACADS* gene: in subject 1, in exons 2 [164 C>T (P55L)] and 9 [1031 A>G (E344G)], and in subject 2, in exons 2 [164 C>T (P55L)] and 3 [323 G>A (G108D)]. The G108D mutation was a novel mutation involving an amino acid (G108) that is highly conserved among *Mus musculus, Danio rerio*, and *Drosophila melanogaster*. The G108D mutation was not detected in 100 unrelated Japanese control individuals, suggesting its potential pathogenic nature.

Because we could not obtain subjects' parents blood sample, the respective cDNAs were prepared and then analyzed by subcloning them into the pGEM-T Easy vector to confirm the mutations. Ten clones were sequenced individually, and in each subject, both mutant alleles were found to be expressed equally (Fig. 1). These results suggest that the two subjects had compound heterozygous mutations in *ACADS*.

SCAD activity analysis

Prior to measuring mutant SCAD enzymatic activity, we confirmed that the assay accurately measured the enzymatic activity of SCAD proteins. Accordingly, *ACADS* cDNA was introduced into a mammalian expression vector, pcDNA, and the resulting expression vector was transfected into HEK293 cells using the calcium phosphate co-precipitation method, as previously reported (Okada et al. 2007). Extracts from 1×10^7 of the transfectants were prepared, and *n*-butyryl-CoA dehydrogenase activity was measured in serially diluted cell samples to obtain a standard curve (Fig. 2a). In HEK293 cells, a linear increase in crotonyl-CoA production was measured in the range of 0.5×10^5–3.0×10^5 cells. Based on the results, extracts from 2×10^5

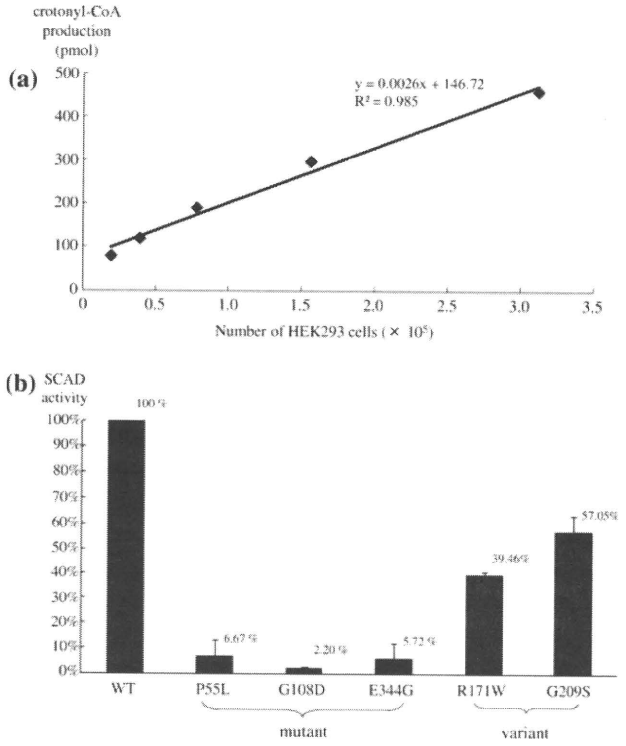

Fig. 2 SCAD enzymatic activity analysis. **a** Butyryl-CoA dehydrogenase activity in crude cell lysates prepared from HEK293 cells transfected with WT *ACADS* plasmid DNA. Standard curve of the enzymatic activity of WT SCAD protein was shown. Based on the results, extracts from 2×10^5 cells were used to analyze SCAD enzymatic activity in all subsequent experiments. **b** SCAD enzymatic activity in HEK293 cells 24 h after transfection with WT or mutant SCAD proteins. WT activity was defined as the 100% value. *Error bars* indicate the standard deviation. The data are the results of triplicate experiments

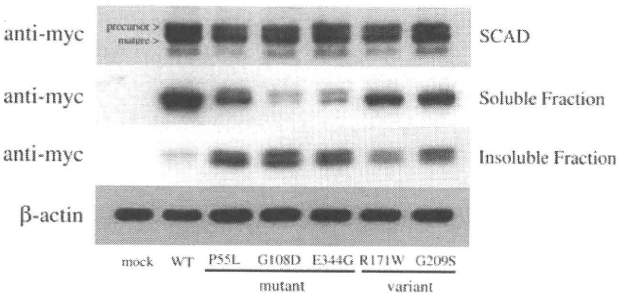

Fig. 3 Western blotting of SCAD proteins. Western blot analysis with an anti-c-Myc antibody to detect SCAD protein. *Top panel* the extracts can be seen to contain equal amounts of SCAD proteins. *Middle* and *lower panels* show the soluble and the insoluble fractions for each of the SCAD proteins. β-Actin served as the control to ensure equal amount of proteins on the filter

cells were used to analyze SCAD enzymatic activity in all subsequent experiments. Each construct was assayed at least three times (Fig. 2b). Expression levels of the recombinant mutant proteins were investigated by Western blot analysis using an anti-c-Myc antibody (Fig. 3).

Compared to the enzymatic activity of the WT SCAD protein, the activities of the G108D and other mutants were <10% (Fig. 2b). The enzymatic profile of the subjects was reproduced by co-transfecting the P55L and E344G mutants (subject 1) or the P55L and G108D mutants (subject 2), and then measuring the enzymatic activities derived from the combined mutant proteins. Low-level activity was detected in each case, analogous to the SCAD activities determined in the subjects (Sup. Fig. 1a). Furthermore, co-transfection of the WT and each of the mutants yielded 60–70% of the normal enzymatic activity, suggesting that these mutants do not influence WT SCAD (data not shown).

Interestingly, an analysis of the common SCAD variants R171W and G209S SCAD showed that their enzymatic activities were 40–60% of the activity measured in the WT (Fig. 2b), whereas co-transfection of R171W and G209S resulted in 50% of the WT activity (Sup. Fig. 1a). According to these results, in individuals harboring these variations, enzymatic activity should be about half that measured in individuals expressing WT SCAD.

In temperature-dependent assay, enzymatic activities of SCAD constructs were entirely lower at 26°C incubation temperature and slightly higher at 41°C incubation temperature than those at 37°C incubation temperature (Sup. Fig. 1b). The whole propensity of decrease of mutants SCAD and variants SCAD against WT SCAD was constant.

Separation of SCAD proteins

To characterize the SCAD mutant proteins, WT, mutant, and variant proteins were purified, and the differences among them were examined. As SCAD mutant proteins are known to misfold and to aggregate (Pedersen et al. 2003) and are thus retained in the insoluble fraction, both the soluble and the insoluble fractions obtained during protein purification were assayed. In the soluble fraction, the amount of mutant SCAD, especially of the G108D mutant, was much less than that determined for the WT (Fig. 3), whereas the amount of variant SCAD in the soluble fraction was only mildly decreased (Fig. 3). As expected, in the insoluble fraction, expression of the mutants was much higher than that of either the WT or the variants (Fig. 3). For each transfectant, the trend was such that the lower the SCAD activity was, the greater was the amount of expression detected in the insoluble fraction.

Immunostaining

Differences in the subcellular localization of the WT and mutant SCAD proteins produced in U2-OS cells were explored by immunostaining. All SCAD proteins were detected in the subcellular region corresponding to the

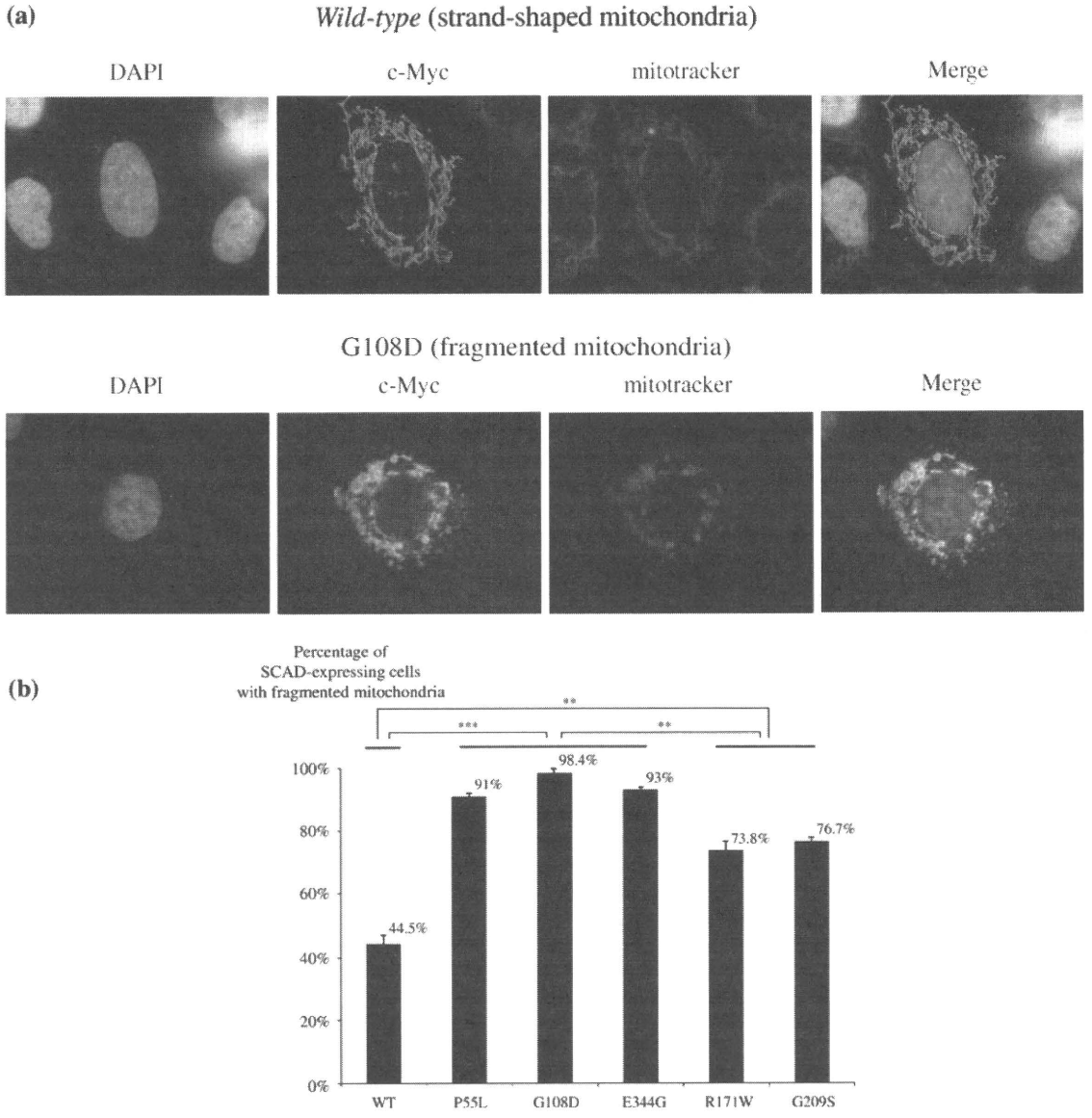

Fig. 4 Immunostaining of WT and G108D SCAD-expressing cells. **a** U2-OS cells transfected with each of the SCAD constructs were immunostained as described in "Materials and methods". Strand-shaped and fragmented mitochondria of cells expressing the WT *ACADS* gene or the G108D mutation were seen, respectively. *Green* showed SCAD protein; *red* showed mitochondria; *blue* showed nuclei. **b** Percentage of SCAD-expressing cells containing fragmented mitochondria. For each transfectant, 300 U2-OS cells were assessed according to mitochondrial shape (***$p < 0.001$, **$p < 0.01$)

mitochondria (Fig. 4a). However, whereas in WT-expressing U2-OS cells, the mitochondria were strand shaped, in cells expressing mutant-SCAD, they were mostly fragmented (Fig. 4a). The mutant proteins were detected in the fragmented mitochondria or spreading within the adjacent cytoplasm. In addition, in many of the mutant-expressing cells the nucleus was deformed. These findings suggest that mutant SCAD proteins are toxic to the mitochondria and/or to the cells themselves (Peng and Jou 2004).

In cells expressing variant SCAD, both strand-shaped and fragmented mitochondria occurred. As in a previous study, the ratio of strand-shaped to fragmented mitochondria was determined in cells containing the WT, mutant, or variant SCAD proteins (Taguchi et al. 2007). The proportion of cells with fragmented mitochondria was much higher in mutant SCAD-expressing cells (Fig. 4b) than in cells expressing the WT (>90 vs. 40%; $p < 0.001$). This trend was strongest in G108D cells and intermediate in the variant cells ($p < 0.01$). These results correlated well with SCAD enzymatic activities, i.e., the lower the SCAD activity of a transfectant was, the higher was the proportion of fragmented mitochondria.

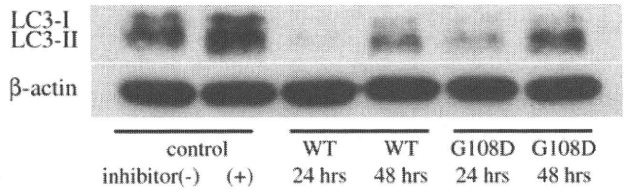

Fig. 5 LC3 assay of WT and G108D SCAD-expressing cells. Western blotting showed that LC3-II, a marker of cellular autophagy, was present in higher amounts in G108D-expressing than in WT-expressing cells. This trend was seen at both 24 and 48 h post-transfection. The amount of protein loaded on the filters was controlled using β-actin

Autophagy in SCAD-overexpressing cells

A recent study showed that mitochondrial fragmentation induces cellular autophagy (Kang and Hwang 2009). Accordingly, we examined whether this was also the case in G108D-expressing cells, in which the severest mitochondrial fragmentation was observed. Autophagy was detected by measuring the expression of LC3-II, a marker of autophagosome formation. At both 24 and 48 h post-transfection, LC3-II expression was stronger in G108D-expressing cells than in cells containing the transfected WT protein (Fig. 5). These results suggested that autophagy was more severely induced in G108D-expressing cells than in those expressing the WT.

Discussion

In this study, compound heterozygous mutations in *ACADS* were identified in two Japanese subjects with SCADD—the first such cases to be diagnosed in Japan. Moreover, in one of them, a novel mutation, G108D, was identified. Enzyme activities of the recombinant mutant SCAD proteins obtained using a transient gene expression system were measured. The activities of the SCAD mutants were found to be <10% of the WT activity (Fig. 2b). Furthermore, co-transfection experiments (P55L and E344G, or P55L and G108D) allowed us to assess the enzymatic activities resulting from the same biallelic mutations detected in the subjects. SCAD activities were also severely impaired in the co-transfectants, showing that the marked SCAD enzymatic defects seen in the two subjects could be precisely measured and characterized by our system. However, to date, neither of these subjects has shown overt clinical symptoms of the disease and, as concluded in previous studies, the genotype–phenotype relationship in SCADD remains unclear. It may well be that the altered SCAD activity may trigger the onset of SCADD under conditions such as starvation or some forms of stress. Therefore, SCADD patients should be followed carefully to obtain a clear understanding of the clinical presentations derived from the enzymatic defect.

The SCAD activities of the R171W and G209S variants were 40–60% in range. Although we also noted an obvious difference in the SCAD activities of the mutants and the variants, the data do not allow us to conclude whether individuals with variant forms of the enzyme will develop clinical symptoms. Another explanation for the pathogenesis of SCADD was proposed by Naito et al. (1989a, b), who suggested that the onset of symptoms is due to the cellular accumulation of abnormal substances (Pedersen et al. 2008). However, it is not known whether, for example, accumulated butyryl-CoA, a substrate of SCAD, or a shortage of its metabolic product plays a role in disease onset, and the pathophysiological implications of the *ACADS* variants and/or mutants remain to be determined.

To further characterize the SCAD mutants and variants, recombinant SCAD proteins were purified, and the soluble and insoluble fractions retained for analysis. The results showed that mutant SCAD proteins were predominately detected in the insoluble fraction, whereas WT protein localized to the soluble fraction (Fig. 3) and variant SCAD was distributed between the two. Generally, the insoluble fraction is considered to contain the cellular bulk of misfolded proteins (Malolepsza 2008). Based on in vitro verifications, Pedersen et al. (2003) suggested that mutant SCAD protein was prone to misfolding and thus to degradation and/or abnormal accumulation. It is also known that misfolded proteins may trigger cellular toxicity (Gregersen et al. 2008; Pedersen et al. 2008) although the molecular mechanism by which this occurs is not well understood. Interestingly, Margineantu et al. (2007) reported that the impairment of heat shock protein (hsp) 90, a molecular chaperone of protein folding, may disturb the ubiquitin–proteasome system, leading to the accumulation of abnormal protein and thus perhaps to mitochondrial fragmentation. As SCAD proteins are folded by hsp 60 (Pedersen et al. 2003), we examined whether the accumulation of SCAD mutant proteins was associated with mitochondrial changes. Immunostaining showed that each of the SCAD proteins (WT, mutants, and variants) was localized to the mitochondria (Fig. 4a), as reported previously (Naito et al. 1989a). Consistent with the conclusions of Margineantu et al., the proportion of cells with fragmented mitochondria was highest in transfectants expressing the mutant SCAD. In addition, the appearance of the fragmented mitochondria correlated well with the decrease in enzymatic activity. To determine whether mitochondrial fragmentation was specific to cells expressing the SCAD mutant proteins, the same experiment was carried out in cells transfected with the WT and K329E mutant MCAD, the most common mutation among patients with MCAD deficiency, and the transfectants were examined by immunostaining

(Sup. Fig. 2). No obvious differences in the mitochondria of WT cells and those expressing the K329E mutation were observed, suggesting that the SCAD mutants impose cellular alterations that are distinct from those due to mutations in the MCAD protein. A previous report suggested that mitochondrial fragmentation impairs mitochondrial homeostasis, and that the degree of mitochondrial damage correlated with the extent of mitochondrial fragmentation (Kim et al. 2007). A close relationship between mitochondrial fragmentation and neuronal degeneration, as well as several diseases, has also been described. For example, in Parkinson disease (PD), more extensive mitochondrial fragmentation is seen in cells exhibiting the PD-causing mutations (Dagda et al. 2009; Itoh et al. 2008; Knott et al. 2008; Lutz et al. 2009; Rodriguez-Hernandez et al. 2009). Therefore, in SCADD, mitochondrial fragmentation may reflect the mitochondrial damage induced by mutant SCAD proteins and may be related to the neuronal symptoms observed in these patients. Recently, pharmacological chaperone therapies against several lysosomal storage diseases by improving folding of mutated enzymes and their stabilities are proposed for future research (Parenti 2009). The same therapies might have the possibility for improving the clinical presentations of SCADD.

Finally, we investigated whether the mitochondrial fragmentation induced by mutated *ACADS* genes results in apoptotic cell death. As obvious differences in apoptotic activities between WT and the G108D mutants were not detected (Sup. Fig. 3), we investigated cellular autophagic activities. Immunoblot experiments showed high-level expression of LC3-II in G108D-expressing cells in which the severest mitochondrial fragmentation was observed. LC3-II is induced during autophagosome formation, and is therefore used as a molecular marker of autophagy, an important mechanism in the maintenance of protein homeostasis. The induction of autophagy has been described in several neuronal and muscle disorders (Bredesen 2008; Malicdan et al. 2008) and in neurodegeneration or neuronal cell death (Cheung et al. 2007; Gorman 2008; Knott et al. 2008). Thus, the induction of LC3-II in cells expressing SCAD mutations suggests a relationship between SCADD and the development of neuronal symptoms.

An association between *Acads* mutations and neurological findings was previously investigated in a mouse model (Tafti et al. 2003). BALB/cByJ mice carrying the G94D mutation in *Acads* showed slow theta oscillations, which may be related to a deterioration of cerebral cortex function. Tafti et al. suggested that a deficiency in the fatty acid metabolism pathway affects theta oscillations. These observations imply a relationship between neuronal disturbances and SCADD in the mouse. In our overexpression experiment using mutant SCAD, the induction of cellular autophagy was observed. So, it is interesting whether asymptomatic subjects have subclinical neurological damage. We think it significant to argue with this possibility. To clarify this point, further investigations including the existence of neurological signs in otherwise asymptomatic subjects are needed, and this might provide an important clue for further clarifying the pathophysiological and clinical features of patients with SCADD.

In this study, we found two female subjects who, as a result of MS/MS newborn screening, were suspected of having SCADD. Both subjects had compound heterozygous mutations, including a novel G108D mutation, in the *ACADS* gene. cDNAs prepared from the peripheral blood of these subjects were used to investigate the activity and solubility of the SCAD enzyme as well as the effects of the mutations on the mitochondria and on cellular autophagy. The expression of mutant SCAD, especially G108D, in transfected cells resulted in a severe decrease in SCAD enzymatic activity, a change in the enzyme's solubility, and the induction of both mitochondrial fragmentation and autophagy. However, as our results were derived from transient gene expression experiments, they cannot be extrapolated to the physiological nature of mutant SCAD proteins in vivo. Further investigations are needed to clarify the relationship between cellular autophagy and neurological symptoms and to determine the implications of our findings with respect to the development of clinical manifestations in patients with SCADD.

Acknowledgments This work was supported by a Grant-in-Aid for Young Scientist (B) No. 20790731 from Japan Society for the Promotion of Science and a grant from the Ministry of Health, Labor, and Welfare of Japan (Chief: Professor Seiji Yamaguchi). This work was carried out at the Analysis Center of Life Science, Hiroshima University.

Conflict of interest statement None declared.

References

Amendt BA, Greene C, Sweetman L, Cloherty J, Shih V, Moon A, Teel L, Rhead WJ (1987) Short-chain acyl-coenzyme A dehydrogenase deficiency. Clinical and biochemical studies in two patients. J Clin Invest 79:1303–1309

Bennett MJ, Gray RG, Isherwood DM, Murphy N, Pollitt RJ (1985) The diagnosis and biochemical investigation of a patient with a short chain fatty acid oxidation defect. J Inherit Metab Dis 8(Suppl 2):135–136

Bhala A, Willi SM, Rinaldo P, Bennett MJ, Schmidt-Sommerfeld E, Hale DE (1995) Clinical and biochemical characterization of short-chain acyl-coenzyme A dehydrogenase deficiency. J Pediatr 126:910–915

Bok LA, Vreken P, Wijburg FA, Wanders RJ, Gregersen N, Corydon MJ, Waterham HR, Duran M (2003) Short-chain Acyl-CoA dehydrogenase deficiency: studies in a large family adding to the complexity of the disorder. Pediatrics 112:1152–1155

Bredesen DE (2008) Programmed cell death mechanisms in neurological disease. Curr Mol Med 8:173–186

Cheung EC, McBride HM, Slack RS (2007) Mitochondrial dynamics in the regulation of neuronal cell death. Apoptosis 12:979–992

Coates PM, Hale DE, Finocchiaro G, Tanaka K, Winter SC (1988) Genetic deficiency of short-chain acyl-coenzyme A dehydrogenase in cultured fibroblasts from a patient with muscle carnitine deficiency and severe skeletal muscle weakness. J Clin Invest 81:171–175

Corydon MJ, Gregersen N, Lehnert W, Ribes A, Rinaldo P, Kmoch S, Christensen E, Kristensen TJ, Andresen BS, Bross P, Winter V, Martinez G, Neve S, Jensen TG, Bolund L, Kolvraa S (1996) Ethylmalonic aciduria is associated with an amino acid variant of short chain acyl-coenzyme A dehydrogenase. Pediatr Res 39:1059–1066

Corydon MJ, Andresen BS, Bross P, Kjeldsen M, Andreasen PH, Eiberg H, Kolvraa S, Gregersen N (1997) Structural organization of the human short-chain acyl-CoA dehydrogenase gene. Mamm Genome 8:922–926

Corydon MJ, Vockley J, Rinaldo P, Rhead WJ, Kjeldsen M, Winter V, Riggs C, Babovic-Vuksanovic D, Smeitink J, De Jong J, Levy H, Sewell AC, Roe C, Matern D, Dasouki M, Gregersen N (2001) Role of common gene variations in the molecular pathogenesis of short-chain acyl-CoA dehydrogenase deficiency. Pediatr Res 49:18–23

Dagda RK, Cherra SJ 3rd, Kulich SM, Tandon A, Park D, Chu CT (2009) Loss of PINK1 function promotes mitophagy through effects on oxidative stress and mitochondrial fission. J Biol Chem 284:13843–13855

Gorman AM (2008) Neuronal cell death in neurodegenerative diseases: recurring themes around protein handling. J Cell Mol Med 12:2263–2280

Gregersen N, Winter VS, Corydon MJ, Corydon TJ, Rinaldo P, Ribes A, Martinez G, Bennett MJ, Vianey-Saban C, Bhala A, Hale DE, Lehnert W, Kmoch S, Roig M, Riudor E, Eiberg H, Andresen BS, Bross P, Bolund LA, Kolvraa S (1998) Identification of four new mutations in the short-chain acyl-CoA dehydrogenase (SCAD) gene in two patients: one of the variant alleles, 511C→T, is present at an unexpectedly high frequency in the general population, as was the case for 625G→A, together conferring susceptibility to ethylmalonic aciduria. Hum Mol Genet 7:619–627

Gregersen N, Andresen BS, Corydon MJ, Corydon TJ, Olsen RK, Bolund L, Bross P (2001) Mutation analysis in mitochondrial fatty acid oxidation defects: Exemplified by acyl-CoA dehydrogenase deficiencies, with special focus on genotype-phenotype relationship. Hum Mutat 18:169–189

Gregersen N, Andresen BS, Pedersen CB, Olsen RK, Corydon TJ, Bross P (2008) Mitochondrial fatty acid oxidation defects—remaining challenges. J Inherit Metab Dis 31:643–657

Itoh T, Ito Y, Ohguchi K, Ohyama M, Iinuma M, Otsuki Y, Nozawa Y, Akao Y (2008) Eupalinin A isolated from *Eupatorium chinense* L. induces autophagocytosis in human leukemia HL60 cells. Bioorg Med Chem 16:721–731

Kang HT, Hwang ES (2009) Nicotinamide enhances mitochondria quality through autophagy activation in human cells. Aging Cell 8:426–438

Kim I, Rodriguez-Enriquez S, Lemasters JJ (2007) Selective degradation of mitochondria by mitophagy. Arch Biochem Biophys 462:245–253

Knott AB, Perkins G, Schwarzenbacher R, Bossy-Wetzel E (2008) Mitochondrial fragmentation in neurodegeneration. Nat Rev Neurosci 9:505–518

Lutz AK, Exner N, Fett ME, Schlehe JS, Kloos K, Lammermann K, Brunner B, Kurz-Drexler A, Vogel F, Reichert AS, Bouman L, Vogt-Weisenhorn D, Wurst W, Tatzelt J, Haass C, Winklhofer KF (2009) Loss of parkin or PINK1 function increases Drp1-dependent mitochondrial fragmentation. J Biol Chem 284:22938–22951

Malicdan MC, Noguchi S, Nonaka I, Saftig P, Nishino I (2008) Lysosomal myopathies: an excessive build-up in autophagosomes is too much to handle. Neuromuscul Disord 18:521–529

Malolepsza EB (2008) Modeling of protein misfolding in disease. Methods Mol Biol 443:297–330

Margineantu DH, Emerson CB, Diaz D, Hockenbery DM (2007) Hsp90 inhibition decreases mitochondrial protein turnover. PLoS One 2:e1066

Naito E, Indo Y, Tanaka K (1989a) Short chain acyl-coenzyme A dehydrogenase (SCAD) deficiency. Immunochemical demonstration of molecular heterogeneity due to variant SCAD with differing stability. J Clin Invest 84:1671–1674

Naito E, Ozasa H, Ikeda Y, Tanaka K (1989b) Molecular cloning and nucleotide sequence of complementary DNAs encoding human short chain acyl-coenzyme A dehydrogenase and the study of the molecular basis of human short chain acyl-coenzyme A dehydrogenase deficiency. J Clin Invest 83:1605–1613

Okada S, Ishikawa N, Shirao K, Kawaguchi H, Tsumura M, Ohno Y, Yasunaga S, Ohtsubo M, Takihara Y, Kobayashi M (2007) The novel IFNGR1 mutation 774del4 produces a truncated form of interferon-gamma receptor 1 and has a dominant-negative effect on interferon-gamma signal transduction. J Med Genet 44:485–491

Parenti G (2009) Treating lysosomal storage diseases with pharmacological chaperones: from concept to clinics. EMBO Mol Med 1:268–279

Pedersen CB, Bross P, Winter VS, Corydon TJ, Bolund L, Bartlett K, Vockley J, Gregersen N (2003) Misfolding, degradation, and aggregation of variant proteins. The molecular pathogenesis of short chain acyl-CoA dehydrogenase (SCAD) deficiency. J Biol Chem 278:47449–47458

Pedersen CB, Kolvraa S, Kolvraa A, Stenbroen V, Kjeldsen M, Ensenauer R, Tein I, Matern D, Rinaldo P, Vianey-Saban C, Ribes A, Lehnert W, Christensen E, Corydon TJ, Andresen BS, Vang S, Bolund L, Vockley J, Bross P, Gregersen N (2008) The ACADS gene variation spectrum in 114 patients with short-chain acyl-CoA dehydrogenase (SCAD) deficiency is dominated by missense variations leading to protein misfolding at the cellular level. Hum Genet 124(1):43–56

Peng TI, Jou MJ (2004) Mitochondrial swelling and generation of reactive oxygen species induced by photoirradiation are heterogeneously distributed. Ann N Y Acad Sci 1011:112–122

Rodriguez-Hernandez A, Cordero MD, Salviati L, Artuch R, Pineda M, Briones P, Gomez Izquierdo L, Cotan D, Navas P, Sanchez-Alcazar JA (2009) Coenzyme Q deficiency triggers mitochondria degradation by mitophagy. Autophagy 5:19–32

Tafti M, Petit B, Chollet D, Neidhart E, de Bilbao F, Kiss JZ, Wood PA, Franken P (2003) Deficiency in short-chain fatty acid beta-oxidation affects theta oscillations during sleep. Nat Genet 34:320–325

Taguchi N, Ishihara N, Jofuku A, Oka T, Mihara K (2007) Mitotic phosphorylation of dynamin-related GTPase Drp1 participates in mitochondrial fission. J Biol Chem 282:11521–11529

Tajima G, Sakura N, Yofune H, Nishimura Y, Ono H, Hasegawa Y, Hata I, Kimura M, Yamaguchi S, Shigematsu Y, Kobayashi M (2005) Enzymatic diagnosis of medium-chain acyl-CoA dehydrogenase deficiency by detecting 2-octenoyl-CoA production using high-performance liquid chromatography: a practical confirmatory test for tandem mass spectrometry newborn screening in Japan. J Chromatogr B Analyt Technol Biomed Life Sci 823:122–130

Tein I, Elpeleg O, Ben-Zeev B, Korman SH, Lossos A, Lev D, Lerman-Sagie T, Leshinsky-Silver E, Vockley J, Berry GT, Lamhonwah AM, Matern D, Roe CR, Gregersen N (2008) Short-chain acyl-CoA dehydrogenase gene mutation (c.319C>T) presents with clinical heterogeneity and is candidate founder

mutation in individuals of Ashkenazi Jewish origin. Mol Genet Metab 93:179–189

van Maldegem BT, Duran M, Wanders RJ, Niezen-Koning KE, Hogeveen M, Ijlst L, Waterham HR, Wijburg FA (2006) Clinical, biochemical, and genetic heterogeneity in short-chain acyl-coenzyme A dehydrogenase deficiency. JAMA 296:943–952

Wanders RJ, Vreken P, den Boer ME, Wijburg FA, van Gennip AH, IJlst L (1999) Disorders of mitochondrial fatty acyl-CoA beta-oxidation. J Inherit Metab Dis 22:442–487

Int J Hematol (2010) 91:245–251
DOI 10.1007/s12185-009-0482-3

ORIGINAL ARTICLE

Significance of immature platelet fraction and CD41-positive cells at birth in early onset neonatal thrombocytopenia

Hirotaka Kihara · Norioki Ohno · Syuhei Karakawa · Yoko Mizoguchi · Rie Fukuhara · Michiko Hayashidani · Shinji Nomura · Kazuhiro Nakamura · Masao Kobayashi

Received: 13 September 2009 / Revised: 25 November 2009 / Accepted: 21 December 2009 / Published online: 16 January 2010

Abstract Early thrombocytopenia is a common hematological abnormality in sick neonates. Here, we examined the relationship between early thrombocytopenia in neonates and parameters associated with thrombopoiesis to identify predictive factors at birth. Two hundred and forty-four neonates admitted to the neonatal intensive care unit were divided into thrombocytopenic ($n = 55$, 23%) and non-thrombocytopenic ($n = 189$, 77%) groups based on platelet counts, which were monitored within 72 h of birth. Immature platelet fraction (IPF) and platelet count at birth were determined simultaneously soon after phlebotomy with an automated hematology analyzer. Megakaryocytes and their precursors positive for CD41 in peripheral blood were examined at birth by flow cytometry. The thrombocytopenic group showed significantly higher IPF percentage and lower percentage of $CD41^+$ mononuclear cells (MNCs) than did the non-thrombocytopenic group ($P < 0.01$). Moreover, the percentage of $CD41^+$ MNCs significantly differentiated neonates with platelet counts $>150 \times 10^3/\mu L$ at birth and nadir platelet count $<150 \times 10^3/\mu L$ over the clinical course from neonates without thrombocytopenia. These observations suggest that the percentage of $CD41^+$ MNCs at birth and IPF percentage are useful predictors of early thrombocytopenia in the majority of sick neonates.

Keywords Thrombocytopenia · Neonate · Immature platelet fraction · Megakaryocyte

H. Kihara · N. Ohno · S. Karakawa · Y. Mizoguchi · R. Fukuhara · M. Hayashidani · S. Nomura · K. Nakamura · M. Kobayashi (✉)
Department of Pediatrics, Hiroshima University Graduate School of Biomedical Sciences, 1-2-3, Kasumi, Minami-ku, Hiroshima 734-8551, Japan
e-mail: masak@hiroshima-u.ac.jp

H. Kihara
e-mail: kihah@mpd.biglobe.ne.jp

1 Introduction

Thrombocytopenia is one of the most common hematological abnormalities in newborn infants, affecting 22–35% of neonates admitted to neonatal intensive care units (NICUs) [1, 2]. Multiple disease processes can cause neonatal thrombocytopenia, and these can be classified as those inducing early thrombocytopenia (<72 h after birth) and those inducing late-onset thrombocytopenia (>72 h). The causes of early thrombocytopenia are well understood: neonatal alloimmune thrombocytopenia [3], maternal immune thrombocytopenic purpura (ITP) or lupus [4], neonatal giant hemangioma [5], perinatal asphyxia, perinatal infection, congenital infection [6], inherited thrombocytopenia caused by reduced platelet production, and congenital errors of metabolism [7]. However, the most frequent cause of early thrombocytopenia is chronic fetal hypoxia, which occurs in infants born to mothers with pregnancy-induced hypertension (PIH) [8] or diabetes [9] and in those who are small for gestational age (SGA) [10]. In the majority of such cases, thrombocytopenia occurs within 3 days and resolves spontaneously within 10 days [1]. The mechanism of transient thrombocytopenia in neonates with these conditions has not yet been elucidated. The method for quantifying reticulated platelets known as the immature platelet fraction (IPF) has been utilized in a variety of clinical conditions such as thrombocytopenic disorders [11–13]. The percentage value and the absolute

value of IPF may be considered to differentiate between insufficient platelet production and increased destruction in patients with thrombocytopenia. Recently, Cremer et al. [13] reported that IPF is a useful parameter to predict the course of neonatal thrombocytopenia. To examine the megakaryopoietic activity in neonates with thrombocytopenia, circulating megakaryocyte progenitor and precursor cells were assessed by progenitor assays for megakaryocyte lineage colony formation [14, 15]. Megakaryopoietic activity in neonates plays an important role in the clinical course of neonatal thrombocytopenia.

In this study, we measured the parameters associated with thrombopoiesis in peripheral blood collected within 24 h after birth.

2 Materials and methods

2.1 Patients

Two hundred and forty-four neonates admitted to the NICUs of Hiroshima University Hospital, Hiroshima Prefectural Hospital, and Hiroshima City Hospital for various indications (e.g., preterm, low birth weight, feeding disability, or respiratory distress) between August 2008 and July 2009 were enrolled in this study. The study was approved by the research ethics committee of Hiroshima University. Exclusion criteria included (1) neonates who received platelet transfusion, (2) those with chromosomal abnormalities, and (3) those in whom complete serial blood cell counts were not examined. One male infant developed sepsis at 3 days old and was excluded from the analysis because he received platelet transfusion. None of the other patients developed early onset sepsis or disseminated intravascular coagulation. After obtaining informed consent from each patient's guardian(s), part of the blood sample was taken for routine diagnostic purposes. All blood samples were obtained within 24 h of birth.

2.2 Measurement of IPF

Immature platelet fraction was analyzed soon after phlebotomy using a fully automated hematology analyzer (XE-2100; Sysmex, Kobe, Japan) with specially designed software. Platelets were divided into mature and immature fractions based on their size and fluorescence intensity. IPF percentage was calculated as the ratio of immature platelets to the total number of platelets.

2.3 Cell preparation and flow cytometry

Aliquots of approximately 250 μL of peripheral whole blood collected in EDTA-2K anticoagulant were used for cell preparation. Red cells were lysed using erythrocyte lysing reagent (Dako, Glostrup, Denmark) and washed twice in phosphate-buffered saline (PBS). The cells were incubated with fluorescein isothiocyanate (FITC)-labeled anti-human CD41 antibody, and the stained cells were analyzed using a FACSCalibur system (Becton–Dickinson Immunocytometry Systems, San Jose, CA). More than 20,000 mononuclear cells (MNCs) were counted, and the percentage positive for CD41 was determined. In some experiments, anti-c-Mpl monoclonal antibody (kindly provided by Kirin Brewery Company, Takasaki, Japan), FITC-labeled anti-human CD42b antibody, and phycoerythrin (PE)-labeled anti-human CD41 antibody were used to confirm that the cells belonged to the megakaryocytic lineage. FITC-labeled anti-human CD41 antibody and FITC-labeled anti-human CD42b antibody were purchased from Dako. PE-labeled anti-human CD41 antibody was purchased from Immunotech (Marseille, France). These analyses were performed on the first day of life.

2.4 Statistical analysis

Statistical significance was determined using the Mann–Whitney U test or Student's t test for data showing a normal distribution. Odds ratio and χ^2 statistics were calculated to quantify the associations between thrombocytopenia and each of SGA, PIH, and premature membrane rupture. Simple regression analysis was performed to examine the relationships among IPF percentage, gestational age, platelet count at birth, absolute IPF value, percentage of $CD41^+$ MNCs, and the nadir of the platelet count. All analyses were performed using StatView software version 5.0 (SAS Institute, Cary, NC), and $P < 0.05$ was considered statistically significant.

3 Results

3.1 Clinical characteristics of the neonates

Two hundred and forty-four neonates (term and preterm) were enrolled in this study. Routine complete blood cell counts were examined serially during the course of the patient's stay in the NICU. Early thrombocytopenia (<72 h of life, platelet count $<150 \times 10^3/\mu L$) was observed in 55 cases (23%). The remaining 189 cases (77%) did not have early thrombocytopenia. Table 1 shows the clinical characteristics of the patients according to group. The birth weight and platelet counts were lower in the thrombocytopenic group than in the non-thrombocytopenic group. The hemoglobin level was higher in the thrombocytopenic group.

Table 1 Patient characteristics

Characteristics	Non-thrombocytopenic group ($n = 189$)	Thrombocytopenic group ($n = 55$)	P value
Gestational age (weeks) (mean ± SD)	35.3 ± 3.6	34.6 ± 4.1	0.214
Birth weight (g) (mean ± SD)	2100 ± 720	1680 ± 730	<0.01
APGAR score (5 min) (mean ± SD)	8.9 ± 1.0	8.6 ± 1.2	0.08
WBC (/μL) (mean ± SD)	13200 ± 6800	11200 ± 6800	0.06
Hb (g/dL) (mean ± SD)	17.2 ± 2.5	18.3 ± 3.1	<0.01
Platelet count (10^3/μL) (mean ± SD)			
At birth	259 ± 47	165 ± 58	<0.01
Nadir	224 ± 47	104 ± 33	<0.01
IPF (%) (mean ± SD)	2.78 ± 1.11 ($n = 153$)	4.31 ± 2.02 ($n = 38$)	<0.01
IPF absolute values (10^3/μL) (mean ± SD)	7.0 ± 2.6 ($n = 153$)	6.4 ± 2.3 ($n = 38$)	0.19
$CD41^+$ MNCs (%) (mean ± SD)	12.2 ± 5.7 ($n = 84$)	7.9 ± 4.4 ($n = 36$)	<0.01

IPF immature platelet fraction, *MNC* mononuclear cell

3.2 Measurement of IPF at birth in non-thrombocytopenic neonates

Figure 1 shows the IPF percentage and platelet count at birth of non-thrombocytopenic neonates. IPF percentage was negatively correlated with gestational age, whereas platelet count at birth was not correlated with gestational age. Overall, IPF percentage in non-thrombocytopenic neonates was 2.78 ± 1.11%. The thrombocytopenic group ($n = 38$) showed significantly higher IPF percentage than the non-thrombocytopenic group ($n = 153$) (Table 1). However, no difference in absolute IPF was found between the two groups.

3.3 Flow cytometric analysis of CD41 in peripheral blood

We examined the percentage of $CD41^+$ MNCs at birth in neonates. Almost all (>95%) of the cells positive for CD41 also expressed c-Mpl, a receptor for thrombopoietin, and CD42b (Fig. 2). The $CD41^+$ MNCs were purified using a FACSAria cell sorting system and assessed using Wright's stain, revealing morphology consistent with that of megakaryocytes and their precursors (data not shown). As shown in Table 1, the percentage of $CD41^+$ cells in the thrombocytopenic group ($n = 36$) was significantly lower than that in the non-thrombocytopenic group ($n = 84$).

3.4 Risk factors for thrombocytopenia

As shown in Table 2, higher rates of SGA and PIH occurred in neonates with thrombocytopenia.

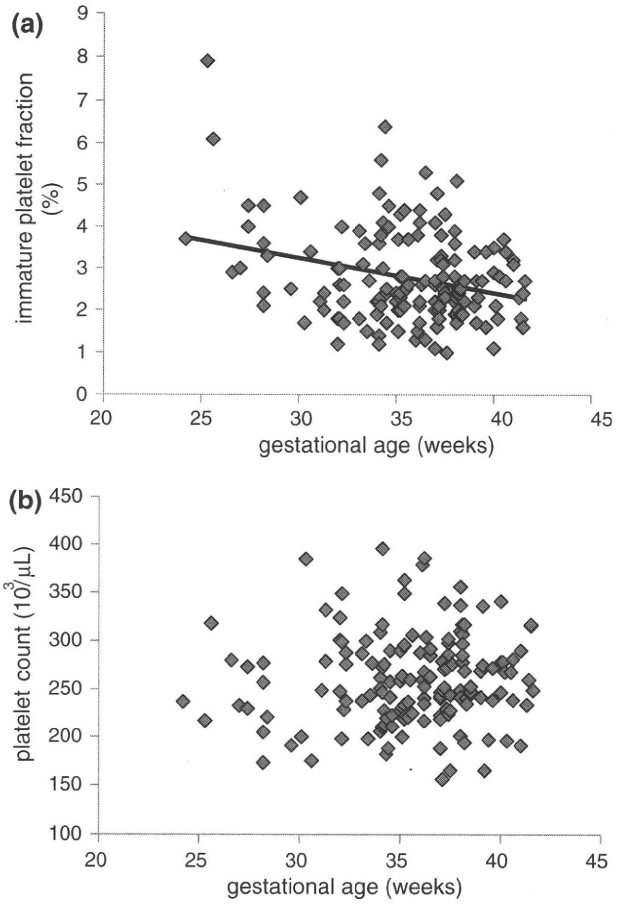

Fig. 1 Immature platelet fraction percentage and platelet count at birth in non-thrombocytopenic neonates ($n = 189$). **a** IPF percentage was negatively correlated with gestational age ($r = -0.28$, $P < 0.01$). **b** Platelet count at birth was not significantly correlated with gestational age ($r = 0.07$, $P = 0.38$)

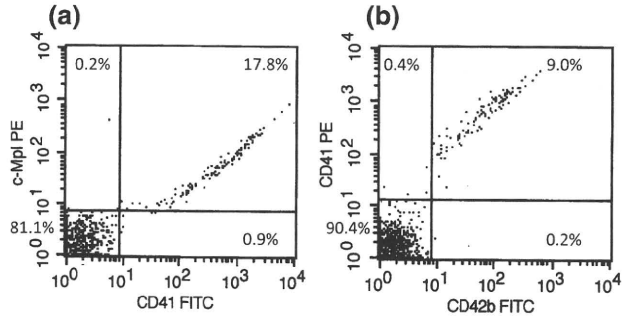

Fig. 2 Flow cytometric analysis of CD41, CD42b, and anti-c-Mpl antibodies. The MNCs positive for CD41 expressed c-Mpl, a receptor for thrombopoietin (**a**), and CD42b (**b**)

Table 2 Risk factors for thrombocytopenia (bivariate analysis)

	Number with thrombocytopenia			
	Risk factor present	Risk factor absent	OR (95% CI)	*P* value
SGA	44/114 (36%)	11/130 (8%)	6.80 (3.3–14.1)	<0.01
PIH	15/39 (38%)	40/205 (20%)	2.58 (1.24–5.35)	0.012
PROM	7/29 (24%)	48/215 (22%)	0.90 (0.36–2.24)	0.83

OR odds ratio, *CI* confidence interval, *SGA* small for gestational age, *PIH* pregnancy-induced hypertension, *PROM* premature rupture of membrane

3.5 Associations between the platelet count nadir and percentage of $CD41^+$ MNCs or IPF values

We examined the relationships between the platelet count nadir and the percentage of $CD41^+$ MNCs or IPF values. As shown in Fig. 3, the platelet count nadir was positively correlated with the percentage of $CD41^+$ MNCs and negatively correlated with IPF percentage at birth, but not with absolute IPF value.

3.6 Analysis of neonates with platelet nadir counts less than $150 \times 10^3/\mu L$

To further examine the risk factors for thrombocytopenia, neonates who were analyzed for both IPF and $CD41^+$ MNCs ($n = 69$) were divided into three groups according to platelet count: group A, platelet count consistently $>150 \times 10^3/\mu L$; group B, platelet count at birth $>150 \times 10^3/\mu L$, but platelet count nadir $<150 \times 10^3/\mu L$; and group C, platelet count consistently $<150 \times 10^3/\mu L$ (Table 3). The percentage of $CD41^+$ MNCs in group B was significantly lower than that in group A (both with platelet counts $>150 \times 10^3/\mu L$ at birth). The percentage of $CD41^+$ MNCs did not differ significantly between groups B and C (both with platelet count nadirs $<150 \times 10^3/\mu L$). No significant differences in absolute IPF value were found among the three groups. No significant differences in IPF percentage were found between groups A and B.

3.7 Relationship between the percentage of $CD41^+$ MNCs and IPF values

We examined the relationship between the percentage of $CD41^+$ MNCs and IPF values. As shown in Fig. 4, the percentage of $CD41^+$ MNCs was positively correlated with absolute IPF value, but not with IPF percentage (data not shown).

4 Discussion

Thrombocytopenia is a common problem in sick neonates [1, 2, 16]. Murray et al. [14, 15] reported that the majority of neonates with early thrombocytopenia showed markedly reduced numbers of circulating megakaryocyte progenitor cells at birth, as determined by cell culture methods for colony-forming unit (CFU)-megakaryocytes (MK) and burst-forming unit (BFU)-MK. In the present study, a significantly lower percentage of $CD41^+$ MNCs at birth was correlated with early transient thrombocytopenia observed in neonates, which was consistent with the findings of Murray et al. [14, 15]. Most of the $CD41^+$ cells expressed CD42b and the thrombopoietin receptor c-Mpl [17] (Fig. 2), supporting the megakaryocytic properties of $CD41^+$ cells. The flow cytometric assay to detect CD41 is a simple, rapid, and reproducible method that requires only small amounts of blood as samples.

The IPF values provided an informative diagnostic method to precisely differentiate the thrombocytopenic disorders. In this study, the IPF percentage of non-thrombocytopenic neonates was negatively correlated with gestational age, which was consistent with a previous report [18]. A significant inverse correlation between platelet count and IPF percentage was reported in patients with immune thrombocytopenic purpura (ITP) [11, 12, 19]. The IPF percentage may reflect the severity of platelet destruction and/or increased platelet production. In neonatal thrombocytopenia, simultaneous IPF and platelet count measurements similarly demonstrated a significant negative correlation between IPF percentage and platelet count [13]. Our results also indicated an inverse relation between platelet count and IPF percentage. However, no significant difference in absolute IPF value was found between thrombocytopenic and non-thrombocytopenic groups. This observation implies that the higher IPF percentage in the thrombocytopenic group may reflect the decrease in number of mature platelets rather than enhanced thrombopoietic activity and the result of insufficient thrombopoiesis. The association between the ratio of

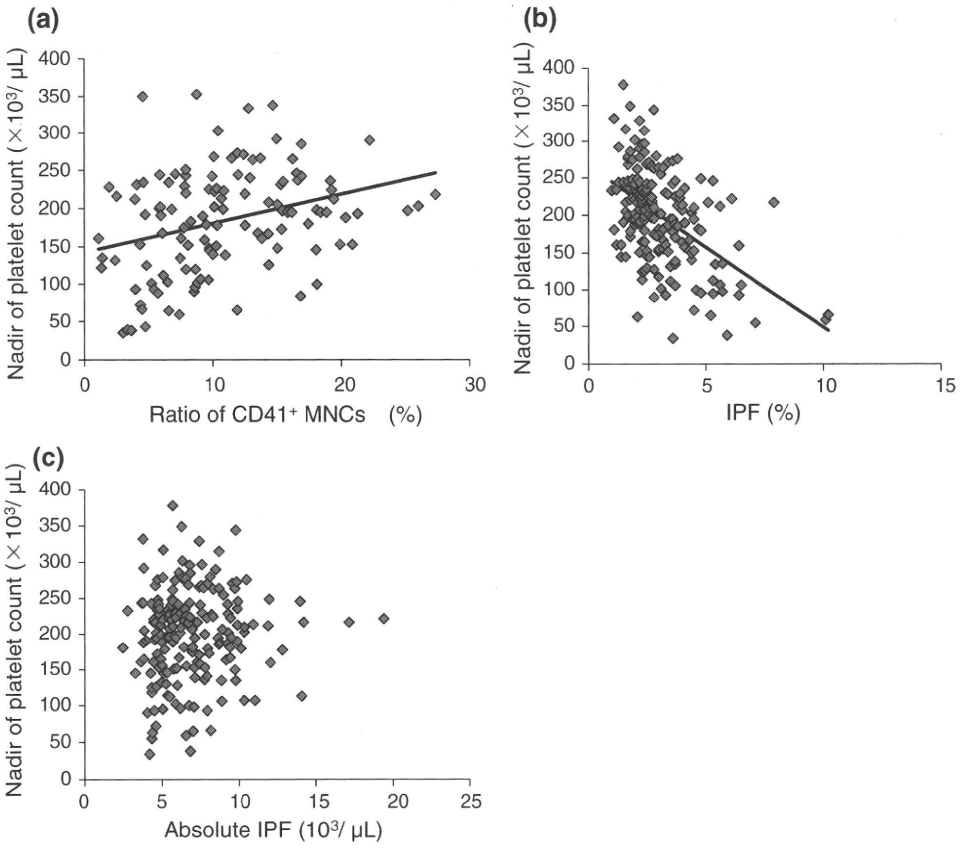

Fig. 3 Associations between the platelet count nadir and the percentage of $CD41^+$ MNCs or IPF values. The platelet count nadir was positively correlated with the percentage of $CD41^+$ MNCs ($r = 0.312$, $P < 0.01$) (**a**) and negatively correlated with IPF percentage at birth ($r = -0.502$, $P < 0.01$) (**b**), but not with absolute IPF value ($r = 0.08$, $P = 0.27$) (**c**)

Table 3 The classification based on platelet count

		n	$CD41^+$ MNCs (%)		Absolute IPF ($10^3/\mu L$)		IPF (%)	
A	Non-thrombocytopenic group	48	12.49 ± 5.66	*	6.77 ± 2.33	NS	2.74 ± 1.09	NS
B	PC at birth > $150 \times 10^3/\mu L$	10	7.75 ± 3.47		6.72 ± 2.52		3.47 ± 1.49	
	PC nadir < $150 \times 10^3/\mu L$			NS		NS		*
C	PC at birth < $150 \times 10^3/\mu L$	11	6.27 ± 2.89		6.15 ± 1.43		5.65 ± 2.69	
	PC nadir < $150 \times 10^3/\mu L$							

Data represent the mean ± SD

* $P < 0.05$

PC platelet count, *NS* not significant

$CD41^+$ MNCs and the absolute IPF value suggests that the ratio of $CD41^+$ MNCs may indicate megakaryopoietic activity. Taken together with the $CD41^+$ cell count and the results of CFU-MK and BFU-MK assays, these observations suggest that the inadequate megakaryopoiesis in neonates represented by low $CD41^+$ cell counts may not lead to compensatory enhancement of thrombopoietic activity; thus, it may result in early thrombocytopenia.

Recently, Sola-Visner et al. [20] quantified the number and size of megakaryocytes in neonate bone marrow samples. The proportion of large megakaryocytes increased significantly in the bone marrow of adults with thrombocytopenia, whereas neonates did not exhibit this response. These findings suggest the potentially limited ability of neonates to increase platelet production in response to increased platelet consumption. Furthermore, Saxonhouse et al. [21] reported the inhibitory effect of hypoxia on proliferation of megakaryocyte progenitors through hypoxia-induced changes in the fetal hematopoietic environment. These findings further support the suggestion that the decreases in circulating megakaryocytes and their precursors in neonates reflect defective megakaryopoiesis.